

REPORT DATE OF PUBLICATION: July 2021
Research Report: UCPRC-RR-2020-01

Concrete Overlay on Asphalt Pilot Project at Woodland SR 113: Construction

Authors:

Angel Mateos, John Harvey, Miguel Angel Millan, Rongzong Wu,
Fabian Paniagua, Jessica Cisneros, and Julio Paniagua

Partnered Pavement Research Center (PPRC) Project Number 3.39 (DRISI Task 3201):
Implementation and Field Performance Evaluation of Concrete Overlay on Asphalt

PREPARED FOR:

California Department of Transportation
Division of Research, Innovation, and System Information
Office of Materials and Infrastructure

PREPARED BY:

University of California
Pavement Research Center
UC Davis, UC Berkeley




TECHNICAL REPORT DOCUMENTATION PAGE

1. REPORT NUMBER UCPRC-RR-2020-01	2. GOVERNMENT ASSOCIATION NUMBER	3. RECIPIENT'S CATALOG NUMBER
4. TITLE AND SUBTITLE Concrete Overlay on Asphalt Pilot Project at Woodland SR 113: Construction		5. REPORT PUBLICATION DATE July 2021
7. AUTHOR(S) Angel Mateos (ORCID 0000-0002-3614-2858), John Harvey (ORCID 0000-0002-8924-6212), Miguel Angel Millan (ORCID 0000-0002-9116-9076), Rongzong Wu (ORCID 0000-0001-7364-7583), Fabian Paniagua (ORCID 0000-0002-2385-4899), Jessica Cisneros, and Julio Paniagua (ORCID 0000-0003-4062-5454)		6. PERFORMING ORGANIZATION CODE
9. PERFORMING ORGANIZATION NAME AND ADDRESS University of California Pavement Research Center Department of Civil and Environmental Engineering, UC Davis 1 Shields Avenue Davis, CA 95616		8. PERFORMING ORGANIZATION REPORT NO. UCPRC-RR-2020-01 UCD-ITS-RR-21-54
12. SPONSORING AGENCY AND ADDRESS California Department of Transportation Division of Research, Innovation, and System Information P.O. Box 942873 Sacramento, CA 94273-0001		10. WORK UNIT NUMBER
15. SUPPLEMENTAL NOTES doi:10.7922/G2PV6HN4		11. CONTRACT OR GRANT NUMBER 65A0788
16. ABSTRACT This report documents the design and construction of a concrete overlay on asphalt (COA) pavement on State Route 113 in Woodland, California, one of the first COA projects in the Caltrans road network. The project site extended over approximately 4 mi. of a two-lane secondary road. The concrete slabs were a half-lane wide (6×6 ft.) and 6 in. thick. The transverse joints were undoweled, but tie bars were installed at all the longitudinal joints. The outside slabs were 2 ft. wider than the interior slabs to provide a concrete shoulder. The project included a section with newly placed, rubberized, gap-graded asphalt mix base. A rapid-strength concrete mixture with Type II/V portland cement designed to be opened to traffic in 24 hours was used for construction of the overlay. The northern part of the project (PM 14.760 to PM 17.580) was built in October and November 2018, while the southern part (PM 11.860 to PM 12.890) was built in April and May 2019. The concrete mixture was produced in a fixed plant and transported in ready-mix trucks 25 mi. to the construction site. A slipform paver was used to consolidate and finish the concrete. A number of the quality control/quality assurance (QC/QA) tests and evaluations summarized in this report were conducted before, during, and after the construction of the concrete overlay. These QC/QA tests and evaluations revealed no major design or construction issues with the concrete overlay, but they did show that the condition of the asphalt base was very poor, particularly in the northern part of the project.		13. TYPE OF REPORT AND PERIOD COVERED Research Report September 2017 to October 2019
17. KEY WORDS rigid pavement, bonded concrete overlay of asphalt, whitetopping, rapid-strength concrete, rubberized asphalt, pavement rehabilitation	18. DISTRIBUTION STATEMENT No restrictions. This document is available to the public through the National Technical Information Service, Springfield, VA 22161	
19. SECURITY CLASSIFICATION (of this report) Unclassified	20. NUMBER OF PAGES 81	21. PRICE None

Reproduction of completed page authorized

UCPRC ADDITIONAL INFORMATION

1. Final	2. VERSION NUMBER 1				
3. PARTNERED PAVEMENT RESEARCH CENTER STRATEGIC PLAN ELEMENT NUMBER 3.39	4. DRISI TASK NUMBER 3201				
5. CALTRANS TECHNICAL LEAD AND REVIEWER(S) Dulce Rufino Feldman	6. FHWA NUMBER CA213201A				
7. PROPOSALS FOR IMPLEMENTATION It is recommended that future concrete overlays on asphalt specifically address the repairs of the asphalt base after the milling operation.					
8. RELATED DOCUMENTS None					
9. LABORATORY ACCREDITATION The UCPRC laboratory is accredited by AASHTO re:source for the tests listed in this report					
10. SIGNATURES					
A. Mateos FIRST AUTHOR	J.T. Harvey TECHNICAL REVIEW	D. Spinner EDITOR	J.T. Harvey PRINCIPAL INVESTIGATOR	D.R. Feldman CALTRANS TECH. LEADS	T.J. Holland CALTRANS CONTRACT MANAGER

Reproduction of completed page authorized

TABLE OF CONTENTS

LIST OF FIGURES	iv
LIST OF TABLES	v
PROJECT OBJECTIVES.....	vii
EXECUTIVE SUMMARY.....	viii
LIST OF ABBREVIATIONS.....	x
LIST OF TEST METHODS AND SPECIFICATIONS USED IN THE REPORT	xi
1 INTRODUCTION.....	1
2 DESCRIPTION OF THE PROJECT	3
2.1 Weather and Traffic	3
2.2 Condition of the Existing Asphalt Pavement	4
2.3 Concrete Overlay on Asphalt Sections.....	11
2.4 Concrete Overlay Mixture.....	15
3 INSTRUMENTATION OF THE SECTIONS	17
3.1 Instrumentation Design and Layout	17
3.2 Sensor-Naming Convention	21
3.3 Sensor Installation.....	23
4 CONSTRUCTION OF THE SECTIONS	29
4.1 Milling the Asphalt Concrete	29
4.2 Asphalt Paving	35
4.3 Construction of the Overlay	37
4.3.1 Construction Timing	37
4.3.2 Preparatory Work	37
4.3.3 Construction Weather Conditions	41
4.3.4 Concrete Paving	44
4.3.5 Concrete Finishing	47
4.3.6 Concrete Curing	48
4.3.7 Joint Saw-Cutting.....	50
4.3.8 Opening to Traffic.....	50
4.3.9 Diamond Grinding.....	51
4.3.10 Transverse Joint Deployment.....	56
4.3.11 Concrete Overlay Thickness	57
5 LABORATORY TESTING OF CONCRETE MECHANICAL PROPERTIES.....	59
6 SUMMARY, CONCLUSIONS, AND RECOMMENDATIONS.....	63
6.1 Summary	63
6.2 Conclusions	63
6.3 Recommendations	64
REFERENCES.....	67

LIST OF FIGURES

Figure 1.1: Layout of the Woodland COA pilot.	2
Figure 1.2: Woodland COA pilot.	2
Figure 2.1: Estimated axle load distribution at Woodland COA pilot.	3
Figure 2.2: Condition of the existing asphalt pavement: cracking.	4
Figure 2.3: Condition of the existing asphalt pavement: rutting.	4
Figure 2.4: Asphalt thickness before milling.	6
Figure 2.5: Cores extracted from between the wheelpaths: Segment A.	7
Figure 2.6 Cores extracted from uncracked areas of the right wheelpath: Segment B.	8
Figure 2.7: Cores extracted from cracked locations in the right wheelpath.	9
Figure 2.8: Deflections measured under FWD loading.	10
Figure 2.9: Layer stiffness backcalculated from FWD testing results.	11
Figure 2.10: Slab size and shoulder configuration.	12
Figure 2.11: COA project test sections.	13
Figure 2.12: COA project experiment design.	14
Figure 3.1: Location of instrumented points.	18
Figure 3.2: Instrumentation layout.	19
Figure 3.3: Fixed DAS set up to collect hygrothermal data from IPs A21, A22, and A31.	20
Figure 3.4: Vibrators of the paving machine.	20
Figure 3.5: Details of instrumentation layout.	21
Figure 3.6: Sensor location identifiers.	22
Figure 3.7: Example of sensor identifiers.	22
Figure 3.8: Installation of the asphalt strain gauges on top of the milled old HMA.	24
Figure 3.9: Set up of RH sensors, VWSG, and thermocouples.	25
Figure 3.10: Rods used for sensor installation.	25
Figure 3.11: Installation of strain gauges.	26
Figure 3.12: Instrumented point A32, right before concrete overlay placement.	27
Figure 3.13: Protection of the sensors during concrete pouring.	27
Figure 4.1: Cold milling machines.	29
Figure 4.2: Milled asphalt thickness deeper than the 6 in. target value.	30
Figure 4.3: Appearance of the asphalt surface after milling.	31
Figure 4.4: Insufficient or and missing asphalt base.	32
Figure 4.5: Asphalt patching on areas with insufficient or missing asphalt base.	32
Figure 4.6: Criteria for rating asphalt condition at the shoulder edge of the roadway.	33
Figure 4.7: Asphalt condition at the shoulder edge of the COA slabs.	34
Figure 4.8: Preparations for asphalt paving.	36
Figure 4.9: Asphalt placement and compaction.	36
Figure 4.10: Examples of cores extracted from the newly placed RHMA-G.	37
Figure 4.11: Concrete paving shifts.	38
Figure 4.12: Dirt on the asphalt surface before concrete paving.	39
Figure 4.13: Tie bar baskets fastened to the asphalt base.	39
Figure 4.14: Manual insertion of tie bars in the plastic concrete.	40
Figure 4.15: Asphalt surface moisture conditioning.	40
Figure 4.16: Air temperatures during concrete paving.	42
Figure 4.17: Air temperature variations during concrete paving.	43
Figure 4.18: Maximum wind speeds during concrete paving.	43
Figure 4.19: Concrete pouring.	44
Figure 4.20: Slipform paver.	44
Figure 4.21: Asphalt surface temperature variation during concrete paving.	45

Figure 4.22: Plastic concrete temperature variation during concrete paving.	46
Figure 4.23: Concrete temperature monitoring, paving Shift 13 (November 14, at night).	47
Figure 4.24: Installation of tie bars instead of dowels at a transverse joint (end of paving Shift 1).	47
Figure 4.25: Surface-finishing and tining.	48
Figure 4.26: Curing compound application.	48
Figure 4.27: Application of the shrinkage-reducing admixture on Section A22.	49
Figure 4.28: Saw-cutting operation.	50
Figure 4.29: Shoulder backfilling.	51
Figure 4.30: Longitudinal smoothness: Segment B.	53
Figure 4.31: Longitudinal smoothness: Segment A.	54
Figure 4.32: Diamond grinding.	55
Figure 4.33: MRI improvement due to grinding.	55
Figure 4.34: Deployed transverse joints.	56
Figure 4.35: Evolution of transverse joint deployment.	57
Figure 4.36: Slab thickness.	58
Figure 5.1: Concrete flexural strength.	60
Figure 5.2: Concrete compressive strength.	61
Figure 5.3: Concrete modulus of elasticity.	61
Figure 5.4: Concrete CTE (at age 42 days).	62
Figure 5.5: Concrete drying shrinkage.	62

LIST OF TABLES

Table 2.1: Concrete Mixture Design	15
Table 3.1: Sensor Types and Characteristics	17
Table 3.2: Sensor Codes.	21
Table 4.1: Concrete Paving Shifts.	38
Table 4.2: SRA Application on Section A22	49

DISCLAIMER

This document is disseminated in the interest of information exchange. The contents of this report reflect the views of the authors who are responsible for the facts and accuracy of the data presented herein. The contents do not necessarily reflect the official views or policies of the State of California or the Federal Highway Administration. This publication does not constitute a standard, specification or regulation. This report does not constitute an endorsement by the California Department of Transportation of any product described herein.

For individuals with sensory disabilities, this document is available in alternate formats. For information, call (916) 654-8899, TTY 711, or write to California Department of Transportation, Division of Research, Innovation and System Information, MS-83, P.O. Box 942873, Sacramento, CA 94273-0001.

ACKNOWLEDGMENTS

The authors of this report would like to thank Caltrans District 3 personnel for the support they provided for the instrumentation, construction monitoring, and initial performance evaluation of the Woodland SR 113 concrete overlay on asphalt (COA) project. The support provided by Resident Engineer Garrett Griffith and Woodland Maintenance facility Supervisor Tony Romero is appreciated. The authors would like to thank the Southwest Concrete Pavement Association as well. This association—in particular, Charles Stuart, executive director—provided continuous support for the design and construction of the Woodland COA pilot. The Caltrans technical review, led by Dulce Rufino Feldman of the Office of Concrete Pavement with oversight by Joe Holland of the Division of Research, Innovation and System Information (DRISI), is highly appreciated. The help that University of California Pavement Research Center staff and students gave in instrumenting the sections and in the monitoring and quality control of the construction is also acknowledged.

PROJECT OBJECTIVES

The primary goal of Partnered Pavement Research Center Strategic Plan Element (PPRC SPE) Project 3.39 is to evaluate the implementation and early field performance of concrete overlay on asphalt (COA) pilot projects. The investigation had a two-fold intention: (1) to help identify how well this treatment works under different climate, traffic, and site conditions and (2) to identify the best practices and standards applicable to the state's climate, materials, and construction work zone practices. This study's main goal will be achieved by completing the following tasks:

1. Document the site conditions and construction of the COA projects, and set a baseline for evaluating the projects' future performance.
2. Gather experience from others, including Caltrans and contractors, involved in COA design and construction. This task includes finding ways to detect any potential design and construction problems associated with the use of this technology in California.
3. Monitor the COA pilot projects' initial performance from the end of construction (May 4, 2019) until August 2020.
4. Evaluate the technology choices that could not be evaluated in PPRC SPE Project 4.58B (Development of Improved Guidelines and Designs for Thin Whitetopping).

The work presented in this report covers Tasks 1 and 2 above. It documents the construction of a COA pavement pilot project on State Route 113 in Woodland, California. The report covers the condition of the pre-existing flexible pavement, milling of the asphalt, and construction of the concrete overlay—including the quality control/quality assurance (QC/QA) testing results. The report also documents the instrumentation built into in the asphalt base and the concrete overlay.

EXECUTIVE SUMMARY

This report documents the design and construction of a concrete overlay of asphalt (COA) pavement pilot project on State Route (SR) 113 in Woodland, California, one of the first projects in the Caltrans road network where this rehabilitation technique has been used. The project extended over roughly four miles of a two-lane road and has two parts. The southern portion, referred to as Segment A (PM 11.860 to PM 12.890), supports traffic of approximately 570 trucks/day (two-way AADTT). The northern portion, referred to as Segment B (PM 14.760 to PM 17.580), supports about 40% as much traffic as the southern part. The project is in California's Inland Valley, a climate region characterized by hot, dry summers and relatively mild, wet winters.

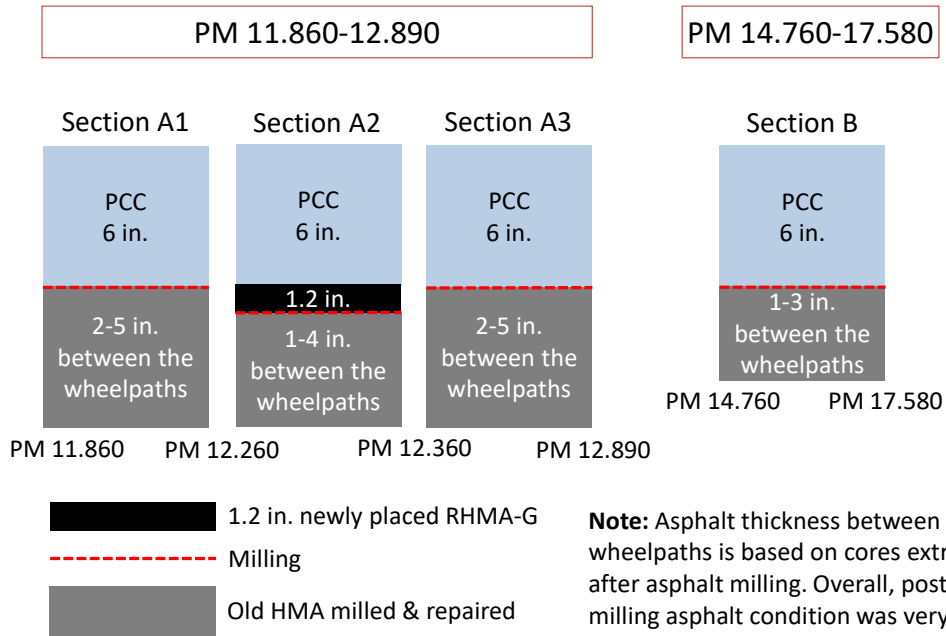
The Woodland SR 113 project design builds on the successful evaluation of a COA project with half-lane width slabs (6×6 ft.) built for an earlier Caltrans research project. The main design features of Woodland SR 113 concrete overlay are the following:

- Transverse joint spacing: 6 ft.
- Slab width: 6 ft. for interior slabs and 8 ft. for exterior slabs (2 ft. widened slabs)
- Slab thickness: 6 in.
- Undoweled (except for transverse construction joints)
- Tie bars at all longitudinal joints

The project included different sections (see the following figure) that were selected to complete a partial factorial design with three factors:

- Asphalt base type: milled old hot mix asphalt (HMA) versus newly placed rubberized gap-graded mix (RHMA-G)
- Asphalt base thickness: around 6 in. in Segment A versus around 3 in. in Segment B
- Curing procedure: standard curing compound versus an advanced curing procedure that consists of the application of a shrinkage-reducing admixture (SRA) spray prior to the application of a standard curing compound

The overlay construction included milling the top 6 in. of the existing asphalt pavement to maintain the original road surface's elevation. It also included paving 0.1 mi. of the project (PM 12.260 to PM 12.360) with 1.2 in. thick RHMA-G. The project's northern part was built in October and November 2018, while its southern part was built in April and May 2019.



COA project test sections.

The mixture used for the overlay construction was a rapid-strength concrete with Type II/V portland cement, a 0.43 water/total cementitious materials ratio, and 15% fly ash. The mixture was designed to provide a 450 psi flexural strength (opening to traffic requirement) in 24 hours. The mechanical characterization of this mix, based on specimens prepared in the field, is presented in this report. The mixture was produced at a fixed plant and delivered by ready-mix trucks to the construction site 25 miles away. A slipform paver was used to consolidate and finish the concrete.

The sections were instrumented with 110 sensors to measure the COA slabs' responses to traffic loading and hygrothermal actions (changes in concrete moisture and/or temperature).

A number of the QC/QA tests and evaluations summarized in this report were conducted before, during, and after the construction of the concrete overlay. These tests and evaluations revealed no major design or construction issues with the concrete overlay, but they did show that the condition of the asphalt base was very poor, particularly in the northern part of the project.

LIST OF ABBREVIATIONS

AADT	Annual average daily traffic
AADTT	Annual average daily truck traffic
AASHTO	American Association of State Highway Transportation Officials
ALR	Areas of localized roughness
COA	Concrete overlay on asphalt
CTE	Coefficient of thermal expansion
DAS	Data acquisition system
FWD	Falling weight deflectometer
GPR	Ground-penetrating radar
HMA	Hot mix asphalt
IRI	International Roughness Index
LTE	Load transfer efficiency
PM	Post mile
MRI	Mean roughness index
PCC	Portland cement concrete
PPRC	Partnered Pavement Research Center
QC/QA	Quality control/quality assurance
RH	Relative humidity
RLT	Real-load testing
SA	Sand-cold mix asphalt
SRA	Shrinkage-reducing admixture
VWVG	Vibrating wire strain gauge
UCPRC	University of California Pavement Research Center
WIM	Weigh-in-motion

LIST OF TEST METHODS AND SPECIFICATIONS USED IN THE REPORT

- AASHTO T 166-13: Standard Method of Test for Bulk Specific Gravity (Gmb) of Compacted Hot Mix Asphalt (HMA) Using Saturated Surface-Dry Specimens
- ASTM C33-18 Standard Specification for Concrete Aggregates
- ASTM C150-19a Standard Specification for Portland Cement
- ASTM C157-17 Standard Test Method for Length Change of Hardened Hydraulic-Cement Mortar and Concrete
- ASTM C260-10a (2016) Standard Specification for Air-Entraining Admixtures for Concrete
- ASTM C309-19: Standard Specification for Liquid Membrane-Forming Compounds for Curing Concrete
- ASTM C494-19 Standard Specification for Chemical Admixtures for Concrete
- ASTM C618-19 Standard Specification for Coal Fly Ash and Raw or Calcined Natural Pozzolan for Use in Concrete
- California Department of Transportation, Standard Specifications, Section 39: Asphalt Concrete, 2015
- California Department of Transportation, Standard Specifications, Section 40: Concrete Pavement, Transportation, 2015
- California Department of Transportation, Standard Specifications, Section 90: Concrete 2015

SI* (MODERN METRIC) CONVERSION FACTORS

APPROXIMATE CONVERSIONS TO SI UNITS				
Symbol	When You Know	Multiply By	To Find	Symbol
LENGTH				
in.	inches	25.40	millimeters	mm
ft.	feet	0.3048	meters	m
yd.	yards	0.9144	meters	m
mi.	miles	1.609	kilometers	km
AREA				
in ²	square inches	645.2	square millimeters	mm ²
ft ²	square feet	0.09290	square meters	m ²
yd ²	square yards	0.8361	square meters	m ²
ac.	acres	0.4047	hectares	ha
mi ²	square miles	2.590	square kilometers	km ²
VOLUME				
fl. oz.	fluid ounces	29.57	milliliters	mL
gal.	gallons	3.785	liters	L
ft ³	cubic feet	0.02832	cubic meters	m ³
yd ³	cubic yards	0.7646	cubic meters	m ³
MASS				
oz.	ounces	28.35	grams	g
lb.	pounds	0.4536	kilograms	kg
T	short tons (2000 pounds)	0.9072	metric tons	t
TEMPERATURE (exact degrees)				
°F	Fahrenheit	(F-32)/1.8	Celsius	°C
FORCE and PRESSURE or STRESS				
lbf	pound-force	4.448	newtons	N
lbf/in ²	pound-force per square inch	6.895	kilopascals	kPa
APPROXIMATE CONVERSIONS FROM SI UNITS				
Symbol	When You Know	Multiply By	To Find	Symbol
LENGTH				
mm	millimeters	0.03937	inches	in.
m	meters	3.281	feet	ft.
m	meters	1.094	yards	yd.
km	kilometers	0.6214	miles	mi.
AREA				
mm ²	square millimeters	0.001550	square inches	in ²
m ²	square meters	10.76	square feet	ft ²
m ²	square meters	1.196	square yards	yd ²
ha	hectares	2.471	acres	ac.
km ²	square kilometers	0.3861	square miles	mi ²
VOLUME				
mL	milliliters	0.03381	fluid ounces	fl. oz.
L	liters	0.2642	gallons	gal.
m ³	cubic meters	35.31	cubic feet	ft ³
m ³	cubic meters	1.308	cubic yards	yd ³
MASS				
g	grams	0.03527	ounces	oz.
kg	kilograms	2.205	pounds	lb.
t	metric tons	1.102	short tons (2000 pounds)	T
TEMPERATURE (exact degrees)				
°C	Celsius	1.8C + 32	Fahrenheit	°F
FORCE and PRESSURE or STRESS				
N	newtons	0.2248	pound-force	lbf
kPa	kilopascals	0.1450	pound-force per square inch	lbf/in ²

*SI is the abbreviation for the International System of Units. Appropriate rounding should be made to comply with Section 4 of ASTM E380. (Revised April 2021)

1 INTRODUCTION

Concrete overlay of asphalt (COA), formerly known as whitetopping, is a pavement rehabilitation technique that consists of placement of a 4 to 7 in. thick concrete overlay on an existing flexible or composite pavement. This technique, an alternative to conventional overlay construction, has been used frequently on highways and conventional roads in several US states as well as in other countries, but its use in California has been very limited.

Under Partnered Pavement Research Center Strategic Plan Element (PPRC SPE) Project 4.58B, the COA technique was successfully evaluated using the accelerated loading applied by a Heavy Vehicle Simulator (2014 to 2017). That research project's main conclusion was that a "well-designed and well-built 6×6 thin bonded concrete overlay placed on top of an asphalt base that is in fair to good condition can potentially provide 20 years of good serviceability on most of California's non-interstate roadways" (1,2). Based on that evaluation, Caltrans decided to implement the technique in the field, and three Caltrans districts proceeded with COA pilot projects. District 11 implemented the COA technique in the rehabilitation of US Interstate 8 (I-8), making it the first use of this technique in the Caltrans road network. Districts 3 and 8 then implemented the technique in the rehabilitation of State Routes (SR) 113 and 247, respectively. This report documents the District 3 COA project, which is in Woodland, California.

The Woodland COA pilot site extended over approximately four miles of SR 113, between PM 11.860 and PM 12.890 and between PM 14.760 and PM 17.580 (Figure 1.1 and Figure 1.2). Between these two sets of post miles, SR 113 is a two-lane road. The northern part of the project, referred to in this report as Segment B (PM 14.760 to PM 17.580), was built during October and November 2018, while the southern part, referred to as Segment A (PM 11.860 to PM 12.890), was built in April and May 2019.

This report documents the construction of the Woodland COA pilot project:

- Chapter 2 describes the project, including the condition of the pre-existing flexible pavement, the COA sections and their design features, and the concrete mixture design.
- Chapter 3 describes the instrumentation embedded in the concrete overlay and the asphalt base. The instrumentation was chosen to measure (1) the structural and hygrothermal responses of the COA slabs under ambient environment actions and (2) the structural response of the COA slabs under the traffic loading.
- Chapter 4 describes the construction of the COA, which included milling, asphalt paving, asphalt surface preparation, paving the concrete overlay, curing, joint saw-cutting, and the grinding needed to meet longitudinal smoothness requirements.
- Chapter 5 includes the results of the laboratory testing conducted on the concrete mix. The testing included an evaluation of the evolution of the concrete's mechanical properties over time.



Figure 1.1: Layout of the Woodland COA pilot.



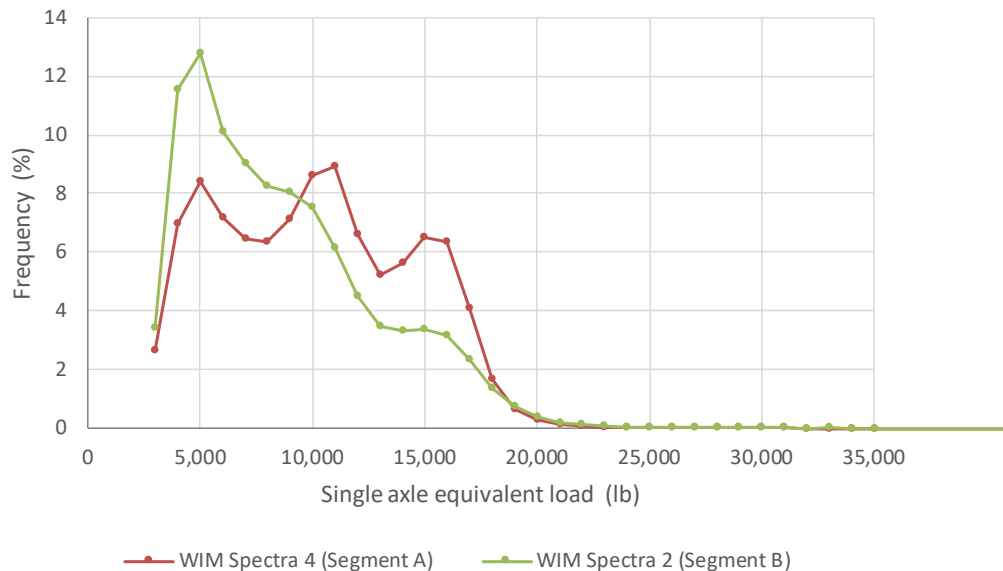
Figure 1.2: Woodland COA pilot.

2 DESCRIPTION OF THE PROJECT

2.1 Weather and Traffic

The city of Woodland, California, is near the state capital, Sacramento, in Climate Region 3, the Inland Valley (IV) (3). This region has a climate that is close to Mediterranean, with hot, dry summers and relatively mild, wet winters. The city's average annual mean temperature is 61°F, with mean monthly values that range from 47°F in December to 77°F in July. Woodland's average annual mean rainfall is 10 in., and its wet season generally runs from November through April while its driest period generally lasts from June to September.

The traffic volume and composition of the project's southern and northern parts (locations shown in Figure 1.1) differ: the southern part (Segment A, PM 11.860 to PM 12.890) supports more and heavier traffic than the northern one (Segment B, PM 14.760 to PM 17.580). The average annual daily traffic (AADT) of Segment A was estimated to be 3,600 (two-way), with 15.9% trucks, and Segment B's estimated AADT was 2,000, with 12.2% trucks. Truck traffic is heavier on Segment A than on Segment B. The truck axle loading distributions of Segments A and B were expected to match Caltrans road network WIM Spectra 4 and 2, respectively (4). The axle load distribution of WIM Spectra 2 and 4 are shown in Figure 2.1.



Note: The single axle equivalent loads (x-axis) are the result of splitting tandem axles in two and tridem axles in three (for example, one tandem becomes two singles with half the load each). The use of single equivalent loads is a simplified way to compare Segment A's WIM spectra with Segment B's.

Figure 2.1: Estimated axle load distribution at Woodland COA pilot.

2.2 Condition of the Existing Asphalt Pavement

Before construction, the condition of the existing asphalt pavement at the project site was relatively poor, mainly due to the presence of alligator cracking in the wheelpaths (Figure 2.2). Cracking was more severe in Segment A than in Segment B, probably due to the greater number of trucks and their heavier weights. Rutting was relatively low, varying from 0.1 to 0.2 in. (Figure 2.3). The data used to generate Figure 2.2 and Figure 2.3 come from the Caltrans Automated Pavement Condition Survey. The evaluation of the existing asphalt pavement's condition included coring and falling weight deflectometer (FWD) testing, as explained below.

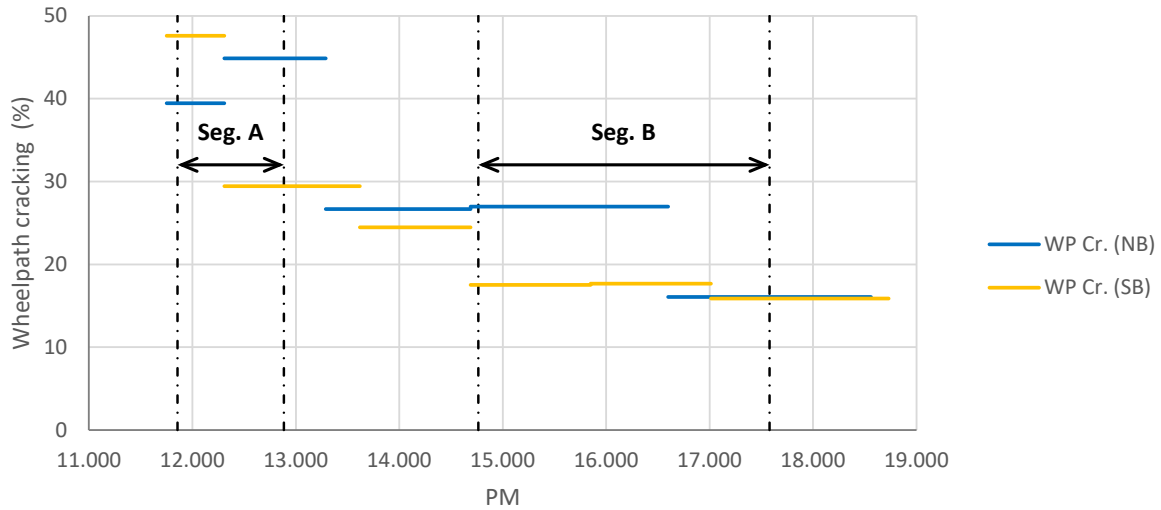


Figure 2.2: Condition of the existing asphalt pavement: cracking.

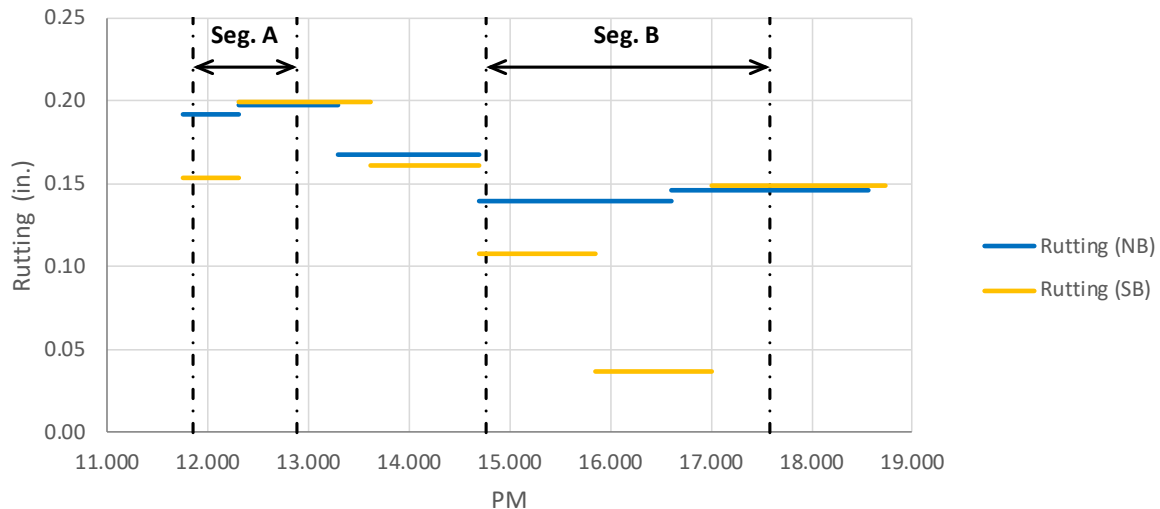


Figure 2.3: Condition of the existing asphalt pavement: rutting.

Based on the data collected in a 2011 Caltrans ground-penetrating radar (GPR) evaluation, the existing pavement's asphalt thickness roughly varied between 13 and 16 in. along Segment A and between 12 and 14 in. along Segment B (Figure 2.4). While cores extracted in 2017 during the COA project's design phase confirmed the GPR measurements in Segment A, they also showed that the actual asphalt thickness along Segment B was roughly 9 to 11 in., somewhat less than the GPR measurements (Figure 2.4). The difference between the two thickness measurements may be attributable to one or more sources. Among them are GPR signal processing errors, moisture that affected the asphalt's dielectric constant, or the presence of an asphaltic material that was in the pavement during the GPR survey but which was destroyed during the coring process. Determining the actual source or sources of the difference would require more research. But whatever the reason, the difference in measurement emphasizes how important it is for an agency to conduct a thorough site investigation of an existing pavement before choosing a rehabilitation type and developing a design for that pavement. And this is true not just for COA: it applies to any rehabilitation project.

All the cores were extracted from spots in or between the wheelpaths. None were extracted at cracked locations or shoulders. The Segment A cores did show frequent delamination and some moisture damage (Figure 2.5) to the asphalt, but the Segment B cores showed the asphalt to be in good condition (Figure 2.6). A second set of cores was extracted from both segments on top of asphalt cracks. These cores showed that cracking had affected the full depth of the asphalt layer and that moisture had produced considerable damage in the lower asphalt lifts (Figure 2.7).

Based on these findings—the asphalt delamination risk that was seen in the Segment A cores (Figure 2.5) and the somewhat better condition of the asphalt in the top lift than in the lower lifts—a recommendation was made that the project include either a minor amount of grinding or no grinding. Ultimately, this recommendation was overridden by another recommendation included in a flooding-risk evaluation that warned against elevating the road surface.

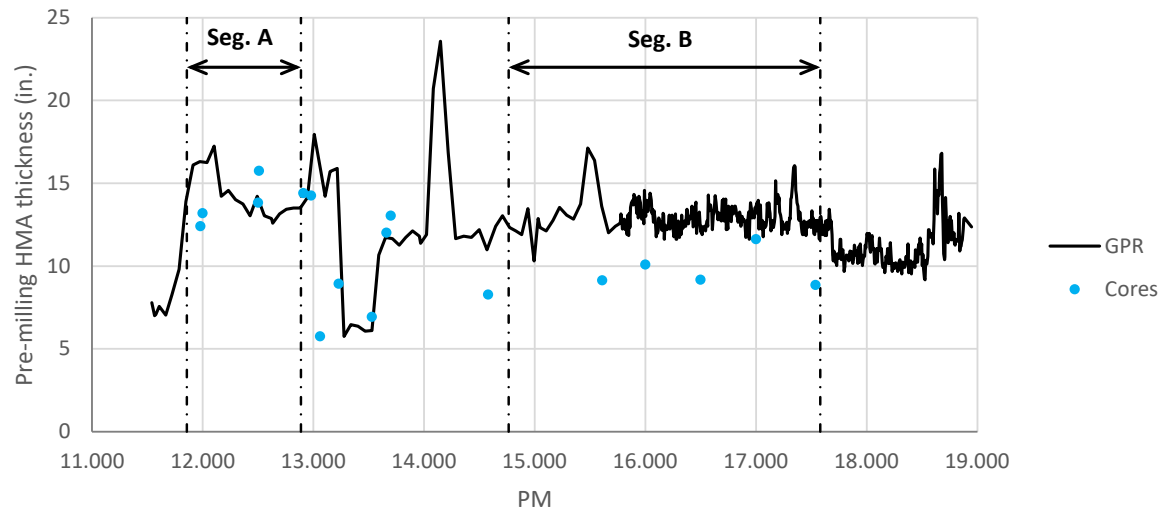


Figure 2.4: Asphalt thickness before milling.



PM 12.000 NB



PM 12.500 NB



PM 12.900 NB



PM 12.000 SB



PM 12.500 SB



PM 12.900 SB

Note: Ruler units are tenths of a foot (not inches).

Figure 2.5: Cores extracted from between the wheelpaths: Segment A.



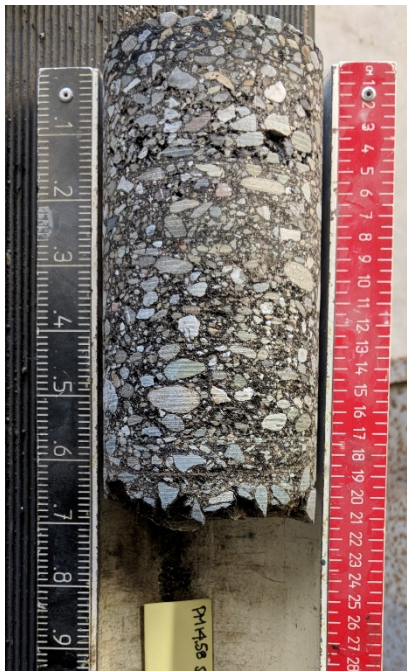
PM 15.600 NB



PM 16.500 NB



PM 17.000 NB



PM 14.600 SB



PM 16.000 SB



PM 17.500 SB

Note: Black/left ruler units are tenths of a foot (not inches); red/right ruler units are centimeters (cm).

Figure 2.6 Cores extracted from uncracked areas of the right wheelpath: Segment B.



Segment A, PM 13.500 NB



Segment A, PM 12.000 SB



Segment A, PM 12.500 SB



Segment B, PM 15.000 NB



Segment B, PM 17.600 NB

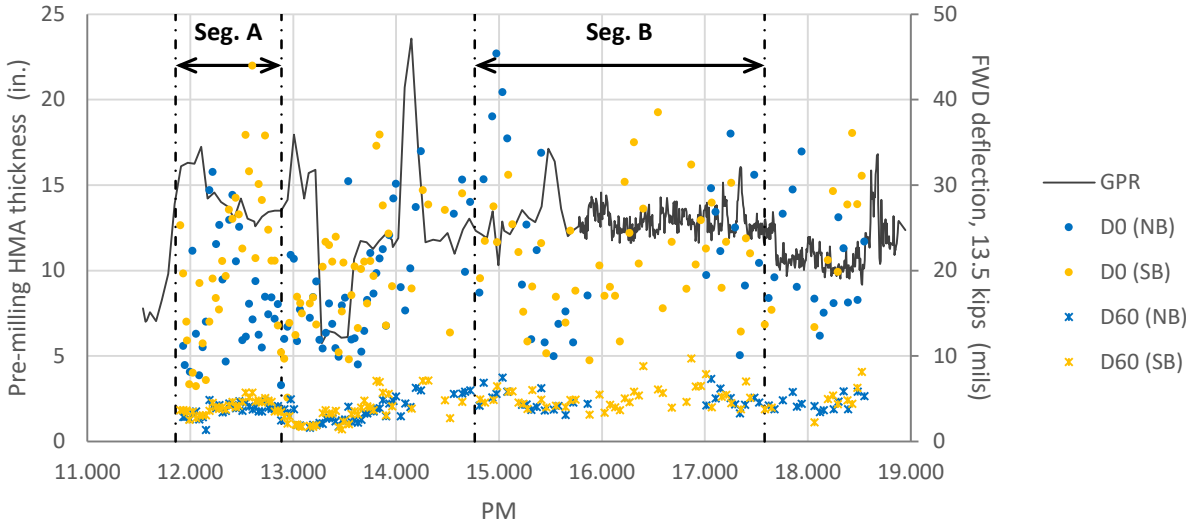


Segment B, PM 17.000 SB

Note: Black/left ruler units are tenths of a foot (not inches); red/right ruler units are centimeters (cm).

Figure 2.7: Cores extracted from cracked locations in the right wheelpath.

The existing asphalt pavement between PM 11.800 and PM 14.000 was evaluated with the FWD on March 30, 2017, and the pavement between PM 14.000 and PM 18.000 was evaluated on October 26, 2017. The evaluations revealed a highly variable bearing capacity, as evidenced by the variability in deflections shown in Figure 2.8. Based on these FWD results, the backcalculated asphalt stiffness varied from around 100,000 to 1.5 million psi, but with no clear pattern related to post mile or asphalt temperature (asphalt temperature varied between 57 and 71°F during the FWD evaluations). The lower limit of the backcalculated stiffness, 100,000 psi, corresponded to an asphalt layer in poor structural condition, while the upper limit, 1.5 million psi, corresponded to an asphalt layer in good structural condition. Subgrade backcalculated stiffness was relatively low, with values ranging from 5,000 to 15,000 psi (Figure 2.9).



Note: D0 and D60 are deflections at, respectively, 0 and 60 in. from the center of the loading plate.

Figure 2.8: Deflections measured under FWD loading.

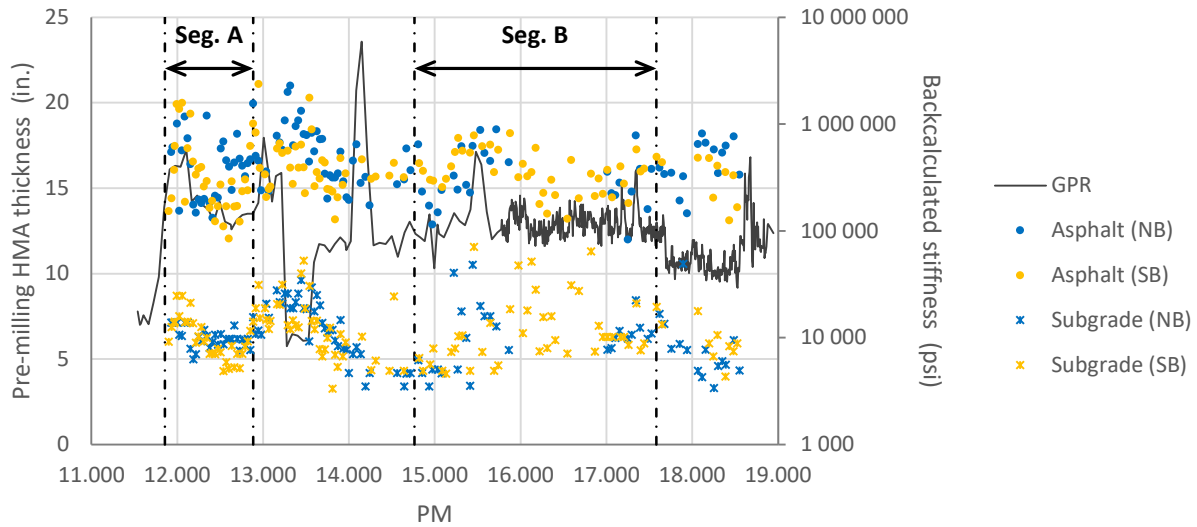


Figure 2.9: Layer stiffness backcalculated from FWD testing results.

2.3 Concrete Overlay on Asphalt Sections

The respective slab sizes selected for the interior and exterior slabs were 6×6 ft. and 6×8 ft. Caltrans adopted this joint spacing configuration (Figure 2.10) to avoid having a joint placed adjacent to the wheelpath. The exterior slabs were widened by 2 ft. to provide a concrete shoulder. The overlay thickness was set to 6 in., based on a mechanistic-empirical design developed using *BCOA-ME* (5). The mechanistic-empirical design assumed 3 in. of asphalt base in fair condition, which does not match the thickness and condition of the asphalt that remained after the milling operation, as described in Section 4.1. During the design phase, the poor condition of the asphalt base and the lack of asphalt at some locations were not anticipated. In an ideal situation, the design procedure selected should be able to account for the actual condition and thickness of the asphalt. *BCOA-ME* assumes that the asphalt’s condition is either good (0% to 8% fatigue cracking) or fair (8% to 20% fatigue cracking), while the actual condition of the milled asphalt base on SR 113 was very poor overall. *BCOA-ME* also assumes a minimum asphalt base thickness of 3 in.

To complete a partial factorial design with three factors, the project’s experimental sections were built using different asphalt base types, asphalt base thicknesses, and curing procedures (Figure 2.11 and Figure 2.12):

- Asphalt base types
 - Milled old hot mix asphalt (HMA); this is the typical asphalt base in COA projects.
 - Newly placed rubberized gap-graded mix (RHMA-G); this base showed excellent performance in the 4.58B project (1).
- Asphalt base thicknesses (after asphalt milling)
 - Approximately 2 to 5 in. between wheelpaths (Segment A).

- Approximately 1 to 3 in. between wheelpaths (Segment B).

(Note: Asphalt thickness is based on cores extracted after the asphalt milling operation.)

- Curing procedures

- Application of standard curing compound.
- Application of shrinkage-reducing admixture (SRA) spray, 8.5 oz./yd², plus standard curing compound. This curing procedure was used on a 42 ft. long (seven slab length) portion of Section A2, in the northbound direction, at PM 12.360. In this report, this small section is referred to as Section A22. The remaining part of Section A2, which was cured with standard curing compound, is referred to as Section A21.

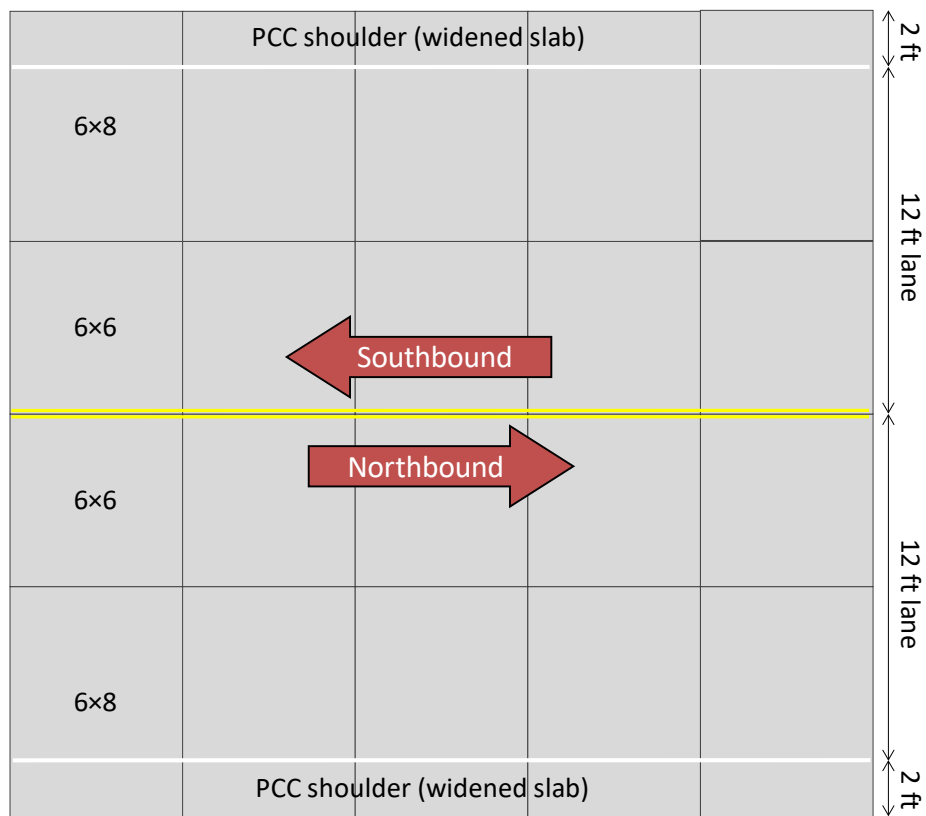


Figure 2.10: Slab size and shoulder configuration.

Initially, concrete overlay thickness was also included as a variable, and the construction of a 0.1 mi. long section with a 5 in. thick portland cement concrete (PCC) overlay was planned between PM 12.360 and PM 12.460. However, after this section was milled, the asphalt surface was 1 in. below the design height. Consequently, the concrete overlay thickness was 6 in., the same as in the rest of the project.

It should be also noted that the asphalt thicknesses in Figure 2.11 and Figure 2.12 are based on cores extracted after the asphalt milling operation. The condition of the asphalt that remained after the milling operation is described in Section 4.1.

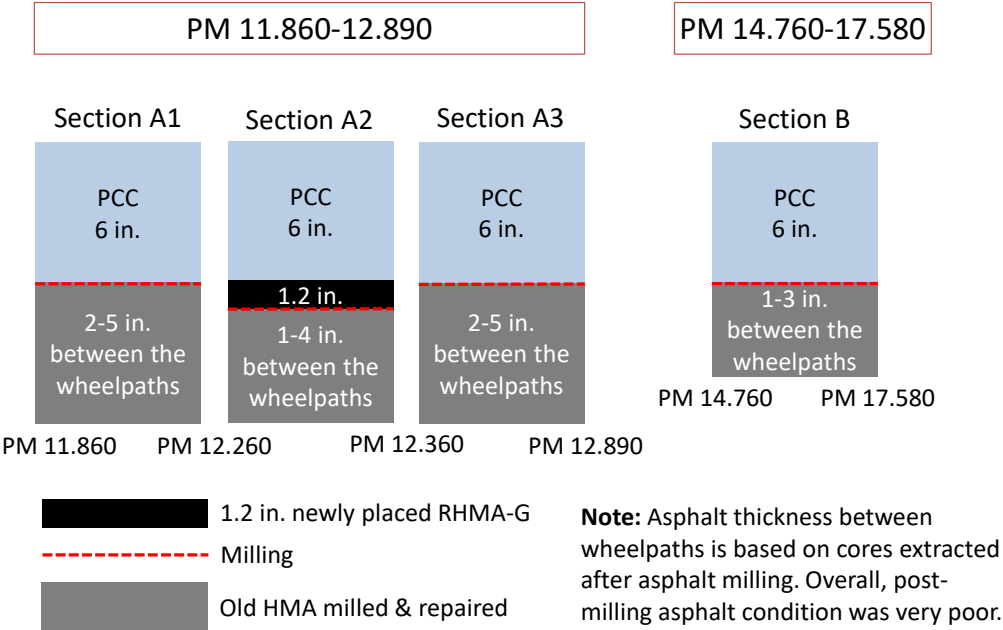


Figure 2.11: COA project test sections.

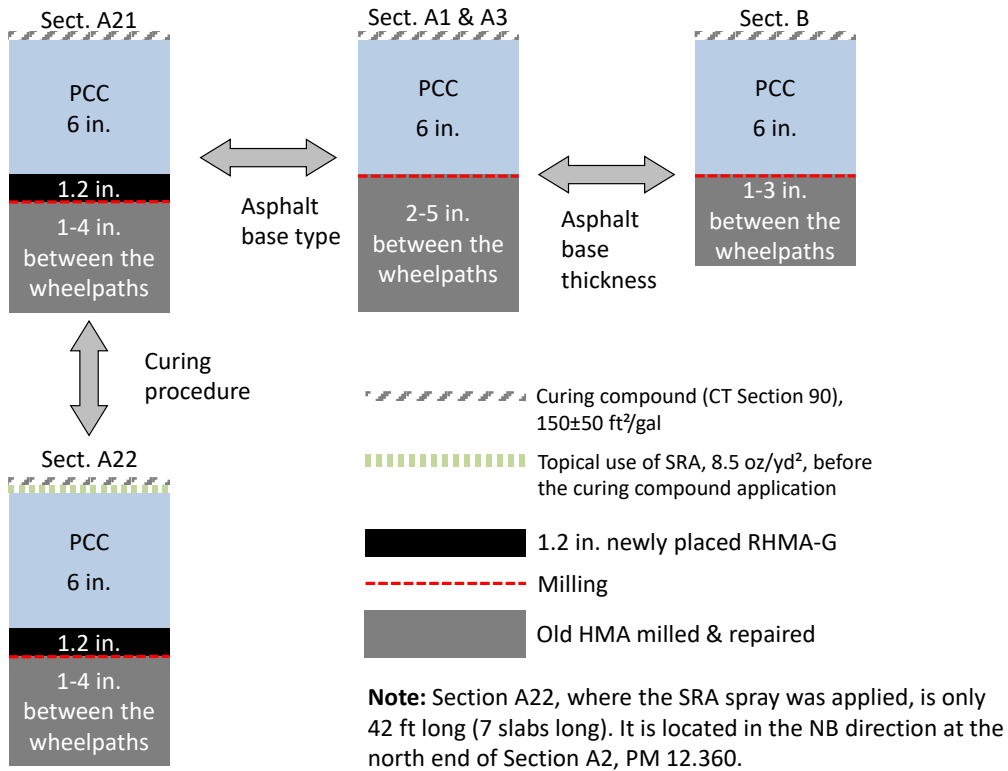


Figure 2.12: COA project experiment design.

The application of a curing compound is the most common curing procedure employed on standard concrete pavements and on concrete overlays. This procedure was required to follow Caltrans Section 90 specifications. More specifically, according to the specification, the curing compound must comply with the ASTM C309 prescriptions for Type 2 (white pigmented) Class B (resin) compounds, and it must be applied at a nominal rate of 150 ft²/gal. (tolerance is ±50 ft²/gal.). The second curing procedure, consisting of the application of an SRA spray prior to the curing compound, followed the successful evaluation of this procedure in the SPE 4.58B research project (1). In its conventional use, SRA is added to the mixing water to reduce the drying shrinkage of concrete. But in this case, the SRA spray was applied to the concrete surface because that is where it would most effectively prevent moisture loss through evaporation. This new curing procedure was attempted in this research project for the first time in the field.

The COA sections also had the following design features:

- Transverse joint spacing of 6 ft.
- No dowel bars at transverse joints, except at construction joints
- Tie bars at all longitudinal joints (between lanes and midlane); two #6 tie bars per slab, placed at mid-slab depth (Caltrans adopted the use of tie bars in all the joints after consultation with the National Concrete Pavement Technology Center)
- Unsealed joints with cuts 1/8 in. wide and 1/3 of slab thickness (2 in.)

2.4 Concrete Overlay Mixture

The concrete mixture was designed to provide flexural strength of 450 psi (project special provisions requirement for opening to traffic) in 24 hours. The mixture proportions are included in Table 2.1. The mixture included Type II/V portland cement, 574 lb./cy, and Class N fly ash (15% total cementitious materials). The ratio of water to total cementitious materials (w/cm) was 0.43. Mixture design slump was 2±0.5 in., which is a low value compatible with slipform paving. The mixture included three types of admixtures: water reducer (3 to 6 oz./cwt [note: cwt stands for 100 lb. of cementitious material]), air entrainer (up to 5 oz./cy), and stabilizer (up to 5 oz./cwt). The admixture supplier was GCP Applied Technologies. The admixtures employed were WRDA[®] 64 water reducer (ASTM C494 Type A and D), Daravair[®] 1000 air entrainer (ASTM C260), and Recover[®] stabilizer (ASTM C494 Type D).

Table 2.1: Concrete Mixture Design

1 cubic yard		
Material	Weight (lb.)	Volume (ft ³)
Cement ASTM C150, Type II/V	574	2.92
Fly ash ASTM C618, Class N	101	0.68
Coarse Aggregate ASTM C33 #57 (1" x #4)	1,350	8.16
Intermediate Aggregate ASTM C33 #8 (3/8" x #8)	437	2.63
Concrete Sand ASTM C33 Sand	1,200	7.14
Air (3±1%)		0.81
Water	291	4.66
Total	3,953	27

The aggregate was extracted from an alluvial deposit in Marysville, California (Teichert Aggregates, Hallwood facility). The mixture was prepared at a fixed plant in Pleasant Grove, California, and transported 25 miles to the construction site in ready-mix trucks.

3 INSTRUMENTATION OF THE SECTIONS

3.1 Instrumentation Design and Layout

The instrumentation of the sections was designed to measure the COA sections' responses to traffic loading and to ambient environmental actions (changes in concrete moisture and/or temperature). In order to measure the response to traffic loading, the sections were instrumented with concrete and asphalt strain gauges. The terms *dynamic* and *traffic* are used to refer to these sensors because they collect data at a very high sampling rate—on the order of thousands of Hz (1,000 samples per second)—under truck traffic or FWD pulse loading.

To measure their responses to ambient environmental actions, the sections were instrumented with vibrating wire strain gauges (VWSGs), thermocouples, and relative humidity sensors. The terms *pseudostatic* and *hygrothermal* are used when referring to these instruments as they collect data at very low sampling rates, on the order of 10^{-3} Hz (one sample every few minutes), under the ambient environmental actions.

Each variable, its corresponding sensor type, and the sensor's make and model number (where known) are presented in Table 3.1. Sensor selection was based on University of California Pavement Research Center (UCPRC) experience with the devices, the expected range of the measured variables, sensor accuracy, the data acquisition system (DAS) requirements, and the ease of installation in the sections.

Table 3.1: Sensor Types and Characteristics

Variable	Sensor Type	Sensor Make and Model
Temperature (concrete and asphalt)	Thermocouple	Omega 5TC-PVC-T-24-180
Dynamic strain (due to traffic loading)	Resistive strain gauge	Tokyo Sokki PML-60 (concrete) Tokyo Sokki PMFLS-60 (asphalt)
Pseudostatic strain (due to hygrothermal actions)	Vibrating wire strain gauge	GeoKon VW Model 4200
Concrete internal relative humidity	Unknown	Campbell Scientific CS215-L

The project was instrumented at four locations (Figure 3.1):

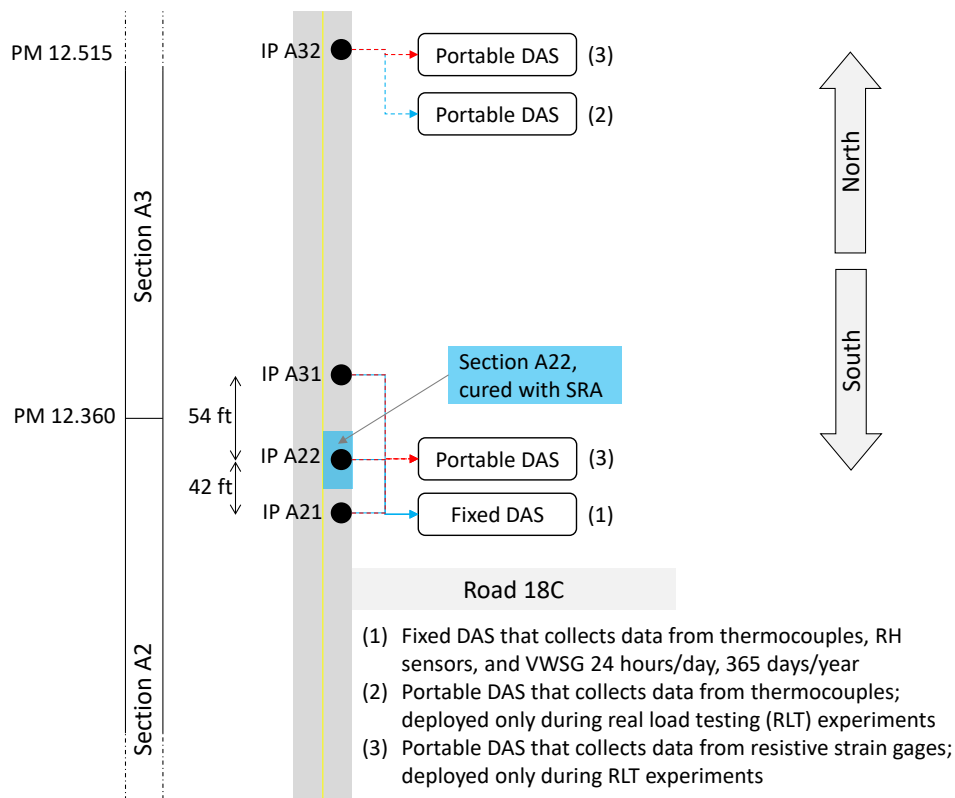
- Instrumented point (IP) A21 in Section A21
- Instrumented point A22 in Section A22
- Instrumented points A31 and A32 in Section A3; IPs A31 and A32 are replicates

Sensors to measure the response under traffic (resistive strain gauges) were installed at all four instrumented points. Sensors to measure the response to ambient environmental actions were also placed at these locations, but the setups at IPs A21, A22, and A31, which included thermocouples, relative humidity (RH) sensors, and VWSGs,

were more comprehensive than at IP A32, which only included thermocouples. The instrumentation layout is shown in Figure 3.2.

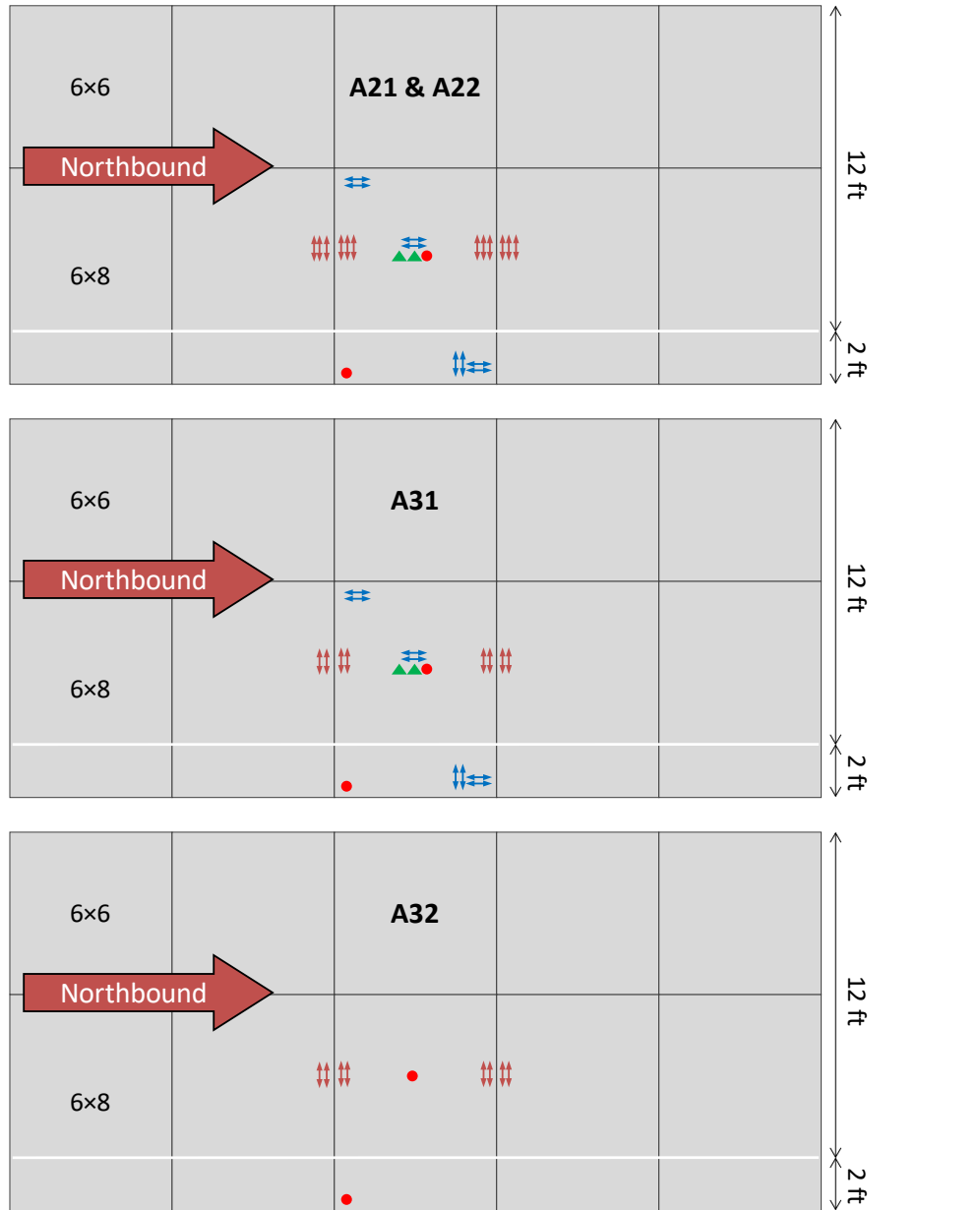
Resistive strain gauges collect data during real-load testing (RLT) experiments. In RLT experiments, a truck with known axle weights runs over the instrumented points. Two RLT experiments were planned for this project, one during summer and one during winter. In both cases, one portable DAS unit would collect data from the resistive strain gauges at IPs A21, A22, and A31, and another would collect the data at IP A32 (Figure 3.1).

The hygrothermal sensors at IPs A21, A22, and A31 were connected to a fixed DAS located near the junction of SR 113 and County Road 18C (Figure 3.3), and that DAS began collecting data every 10 minutes on the day before construction of the concrete overlay. The hygrothermal sensors (thermocouples) at IP A32 were connected to a portable DAS only during the RLT experiments (Figure 3.1).



Note: The figure is not to scale.

Figure 3.1: Location of instrumented points.



- 5 thermocouples (4 in concrete slab + 1 in asphalt base):
 - 0.4 in. depth
 - 1 in. depth
 - 2.4 in. depth
 - Bottom concrete slab
 - Asphalt base, 1.2 in. below asphalt surface
- ≡≡≡ 3 Dynamic Strain Gages :
 - 1 in. below slab surface
 - 1 in. above slab bottom
 - Interface RHMA-G/Old HMA
- ≡≡ 2 Dynamic Strain Gages :
 - 1 in. below slab surface
 - 1 in. above slab bottom
- ⇔⇔ 2 VWSG:
 - 1 in. below slab surface
 - 1 in. above slab bottom
- ▲ RH sensor, 1 in. below slab surface

Note: Section A31 PCC thickness was planned to be 5 in., and sensor heights were set accordingly. However, due to a construction issue, that final height was 6 in. Consequently, the sensors located at the top of the slab ended up 1 in. deeper than expected (this is applicable to top strain gauges, relative humidity sensors, and three top thermocouples).

Figure 3.2: Instrumentation layout.



Figure 3.3: Fixed DAS set up to collect hydrothermal data from IPs A21, A22, and A31.

The paving machine was equipped with a set of vibrators that may have impacted the sensors embedded in the concrete overlay (Figure 3.4). For this reason, the transverse locations of some sensors (that is, perpendicular to the direction of traffic) were adjusted slightly to keep them out of vibrators' path. The right wheelpath sensors, whose transverse location was originally planned to be 5 ft. (60 in.) from the shoulder edge of the slabs, were moved 2 in. toward the shoulder. Similarly, the corner sensors were moved 2 in. in the transverse direction. The final transverse positions of the different sensors are shown in Figure 3.5.



Figure 3.4: Vibrators of the paving machine.

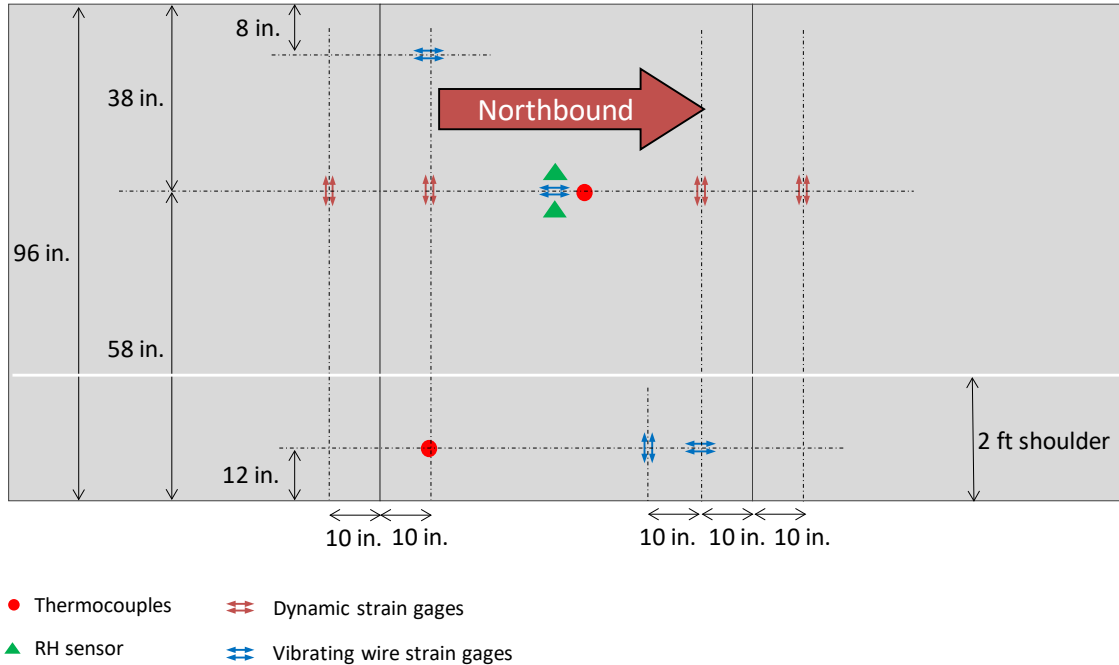


Figure 3.5: Details of instrumentation layout.

3.2 Sensor-Naming Convention

Each sensor was assigned a unique identifier composed of four parts, each separated by a period (for example, Therm.A21.S13=C.10 refers to the thermocouple located in Section A21, Slab 13, at the center of the slab, at 10 tenths of an inch depth). The following describes how this identifier was developed:

1. The first part of the identifier indicates the sensor type and direction (where applicable). The codes for the different types of sensors are shown in Table 3.2.

Table 3.2: Sensor Codes

Codes	Sensor Type	Direction
Therm	Thermocouple	Not applicable
DySG	Resistive strain gauge ("Dy" stands for dynamic)	Transverse (T) Longitudinal (L)
StSG	Vibrating wire strain gauge ("St" stands for pseudostatic)	
RH	Relative humidity sensor	Not applicable

2. The second part of the identifier indicates the instrumented point (for example, A21, A22, etc.).
3. The third part of the identifier indicates the sensor location, which is indicated by the slab number following the letter S, and by the sensor's location—C for center, R for right, and L for left—within the slab (Figure 3.6). For example, S13=C indicates the center of Slab 13.

- a. Slab numbers have been assigned as indicated in Figure 3.6 (left). Note that this assignment assumes a virtual section that is five slabs long.
- b. The sensor's location within the slab is indicated with a symbol and a letter, as indicated in Figure 3.6 (right).

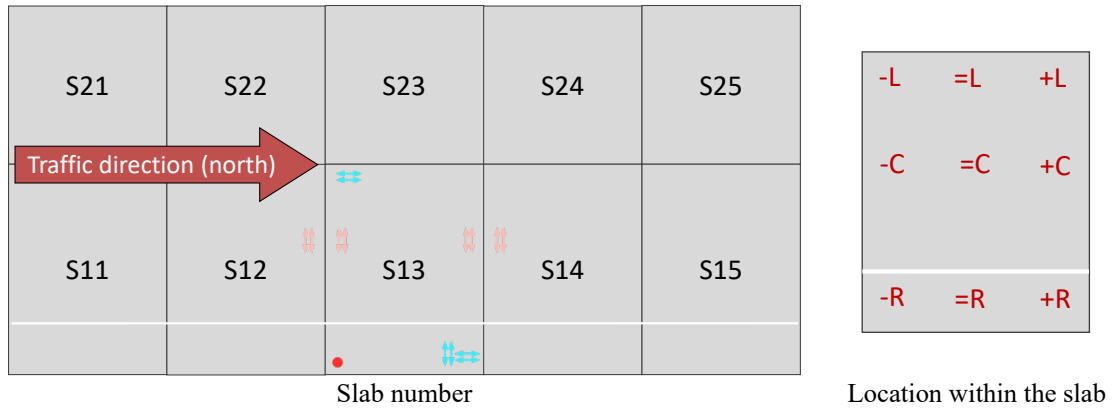


Figure 3.6: Sensor location identifiers.

- 4. The fourth part of the identifier indicates the theoretical depth of the sensor, in tenths of an inch. A lowercase letter b is used to indicate a replicate sensor.

Figure 3.7 includes examples of sensor identifiers.

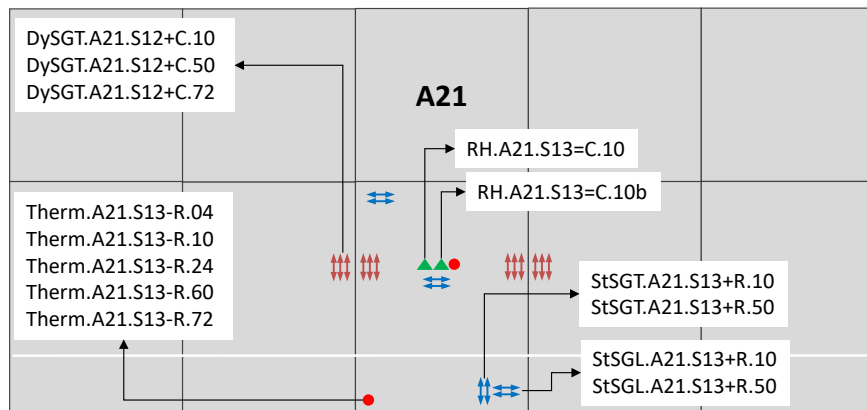


Figure 3.7: Example of sensor identifiers.

3.3 Sensor Installation

Some sensors were installed in the asphalt while others were installed in the concrete (Figure 3.2):

- The sensors installed in the asphalt included thermocouples located 1.2 in. below the asphalt surface and the asphalt strain gauges located at the interface between the newly placed RHMA-G and the milled old HMA in IPs A21 and A22.
- The sensors embedded in the concrete included the rest of the thermocouples and resistive strain gauges, the VWSGs, and all the RH sensors.

The asphalt strain gauges were placed on top of the milled old HMA at IPs A21 and A22. Sand-cold mix asphalt (SA) was used to fix the strain gauge cables to the old HMA surface and to prepare a bed for the strain gauges (Figure 3.8, top left and top right). In addition to fixing the gauges to the milled old HMA surface, the SA bed prevented the uneven milled surface from punching through the gauges during the RHMA-G compaction. The gauges and cables were covered with hot RHMA-G right before the asphalt paver arrived at their location (Figure 3.8, bottom right). The goal of this operation was to prevent the gauges from moving during the extension of the RHMA-G overlay.

The asphalt thermocouples were inserted into a 1.2 in. long hole drilled into the asphalt. The thermocouples installed at the bottom of the concrete overlay were placed directly on top of the asphalt base. The rest of them were attached to a wooden rod at the desired heights, as shown in Figure 3.9. In order to secure the wooden rod to the asphalt base, the rod was inserted into a hole drilled into the asphalt and fitted with a wood base that was glued with epoxy to the asphalt surface (Figure 3.10).

The RH sensors were installed using a rod similar to the one used with the thermocouples (Figure 3.9). The RH rod included a metal jacket and a horizontal nail that served as chair for the RH sensor. The RH sensors were secured to the nails with zip ties.

The resistive strain gauges and VWSGs were installed using rods similar to those used with the RH sensors (Figure 3.11). Each strain gauge rod included two horizontal nails that served as chairs for the upper and lower strain gauges (Figure 3.10). The strain gauges were secured to the nails by zip ties.



Fixing strain gauge cable with sand-cold mix asphalt



Strain gauges placed on SA bed (to prevent the milled surface from punching through the gauge during the RHMA-G compaction)



Strain gauge and cable protection until RHMA-G placement



Hot RHMA-G placed over the strain gauges and cables right before the RHMA-G extension

Figure 3.8: Installation of the asphalt strain gauges on top of the milled old HMA.



RH sensors (silver sensors with the white cap, back), VWSG (blue, second from back), and thermocouple rod (black, right)

Figure 3.9: Set up of RH sensors, VWSG, and thermocouples.



Thermocouple rod (left), strain gauge rods (center and right)

Figure 3.10: Rods used for sensor installation.



VWSG



Resistive strain gauges

Figure 3.11: Installation of strain gauges.

The final steps in the sensor installation procedure were (1) to check the sensors' labels to ensure correct placement, (2) to cut off the zip ties and sensor labels, (3) to affix the sensor cables to the asphalt surface with epoxy (Figure 3.12), and (4) to protect the sensors during concrete placement. That last step was accomplished by a crew from the UCPRC. First, each person carefully shoveled concrete around the sensors, then used the shovel to prevent the devices from receiving the direct impact of the concrete poured from the truck's discharge chute, as reflected in Figure 3.13 (left). Once sensors were engulfed by the concrete, crewmembers consolidated the concrete by hand around them using a 1 in. diameter manual vibrator, as reflected in Figure 3.13 (right). As a result of this protective approach, only one VWSG and two resistive strain gauges were lost among all the sensors installed.



All sensors fixed to rods or chairs, zip ties tips and sensor labels cut, cables fixed with epoxy to the asphalt base.

Figure 3.12: Instrumented point A32, right before concrete overlay placement.



A UCPRC crew shovels concrete around the sensors; then uses the shovels to protect them from the direct impact of the concrete poured from the truck's discharge chute



Consolidating the concrete around the sensors

Figure 3.13: Protection of the sensors during concrete pouring.

4 CONSTRUCTION OF THE SECTIONS

4.1 Milling the Asphalt Concrete

The asphalt surface milling took place on October 20, 2018, on Segment B and on April 24, 2019, on Segment A (see segment layout in Figure 1.1). Two different cold milling machines were used for each segment (Figure 4.1). Each milling machine pass removed an asphalt band approximately 6 to 8 ft. wide. The target depth (6 in.) was achieved on a single pass. At most locations, the actual milled depth was 1 to 2 in. deeper than the 6 in. target value (Figure 4.2). After the milling operation, several passes of a mechanical broom cleaned the milled surfaces.



Segment A



Segment B

Figure 4.1: Cold milling machines.

Overall, the milling operation revealed an asphalt base in poor condition. Cracking and areas of delamination were present all over the project (examples in Figure 4.3). Further, in many locations the milling operation either left an insufficient asphalt base or entirely removed the asphalt base at the shoulder edge of the roadway, as shown in the photographs in Figure 4.4. As can be seen in those photographs, the width of the available milled asphalt base was too narrow to provide a continuous support under the COA slabs, which would leave the shoulder edge of the exterior slabs resting on the aggregate subbase instead of the milled asphalt base. This structural condition may eventually cause longitudinal cracking of the concrete overlay. At some locations, the shoulder edge of the milled roadway was paved with asphalt to provide a uniform support for the COA slabs (Figure 4.5).



Figure 4.2: Milled asphalt thickness deeper than the 6 in. target value.



Segment B: Asphalt cracking and areas with delamination



Segment A: Asphalt cracking and areas with delamination

Figure 4.3: Appearance of the asphalt surface after milling.



Example on Segment A



Example on Segment B

Note: The exterior concrete slabs are 6×8 ft. (widened into the shoulder, Figure 2.10). The asphalt base was supposed to extend 8 ft. outside the midlane longitudinal joint. However, at many locations the asphalt base did not extend that far.

Figure 4.4: Insufficient or and missing asphalt base.



See asphalt patch on the right side of the picture



Figure 4.5: Asphalt patching on areas with insufficient or missing asphalt base.

A visual survey was conducted to quantify the condition of the milled asphalt base at the shoulder edge of the roadway. In this survey, a rating between -2 and +2 was assigned to each 100 ft. long roadway segment. A -2 rating refers to a scenario where an insufficient asphalt base width ends about 2 ft. inside the lane-shoulder line while a +2 rating refers to a scenario where the asphalt base extends 2 ft. into the shoulder, as shown in Figure 4.6. A +2 rating was also assigned to segments where the shoulder had been paved with asphalt (Figure 4.5) after milling. The results of the visual survey are shown in Figure 4.7.

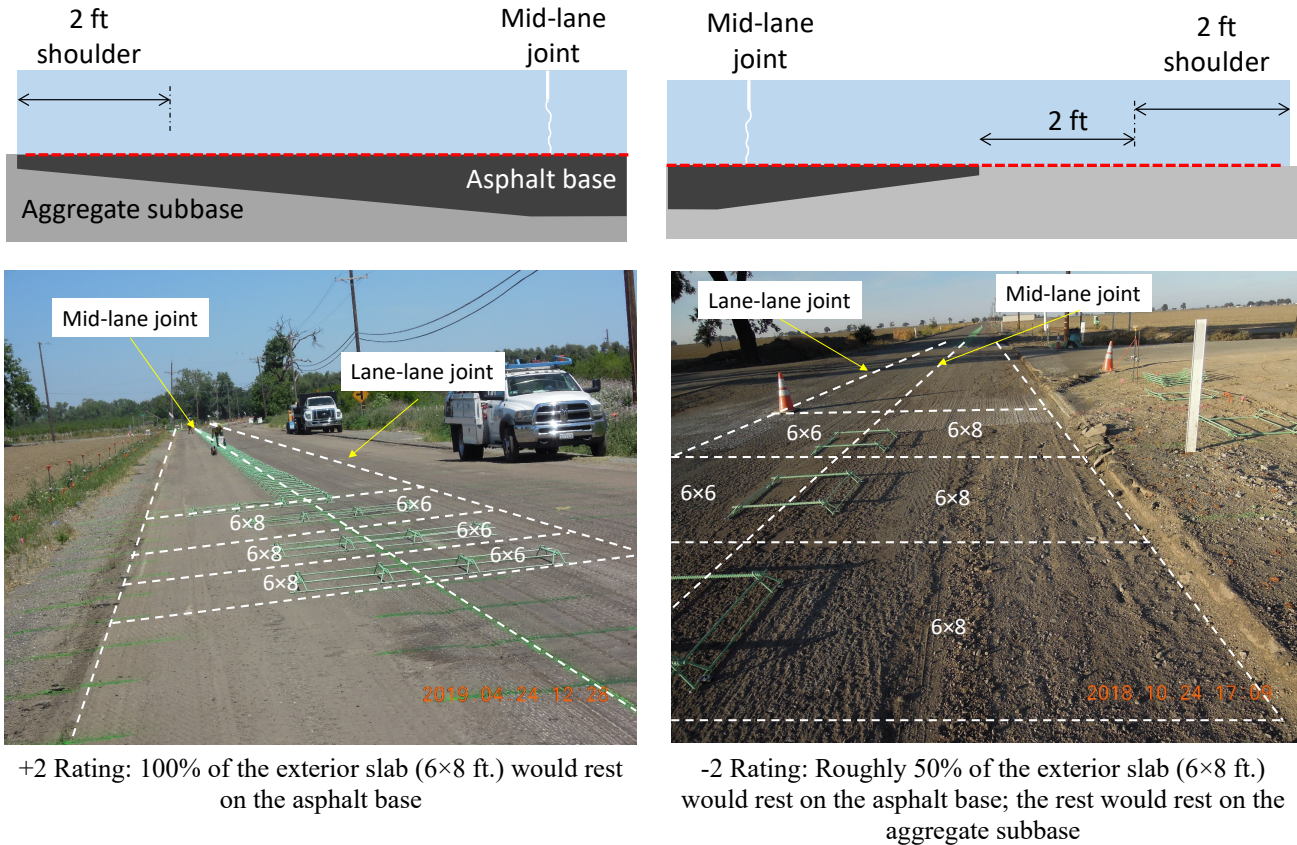
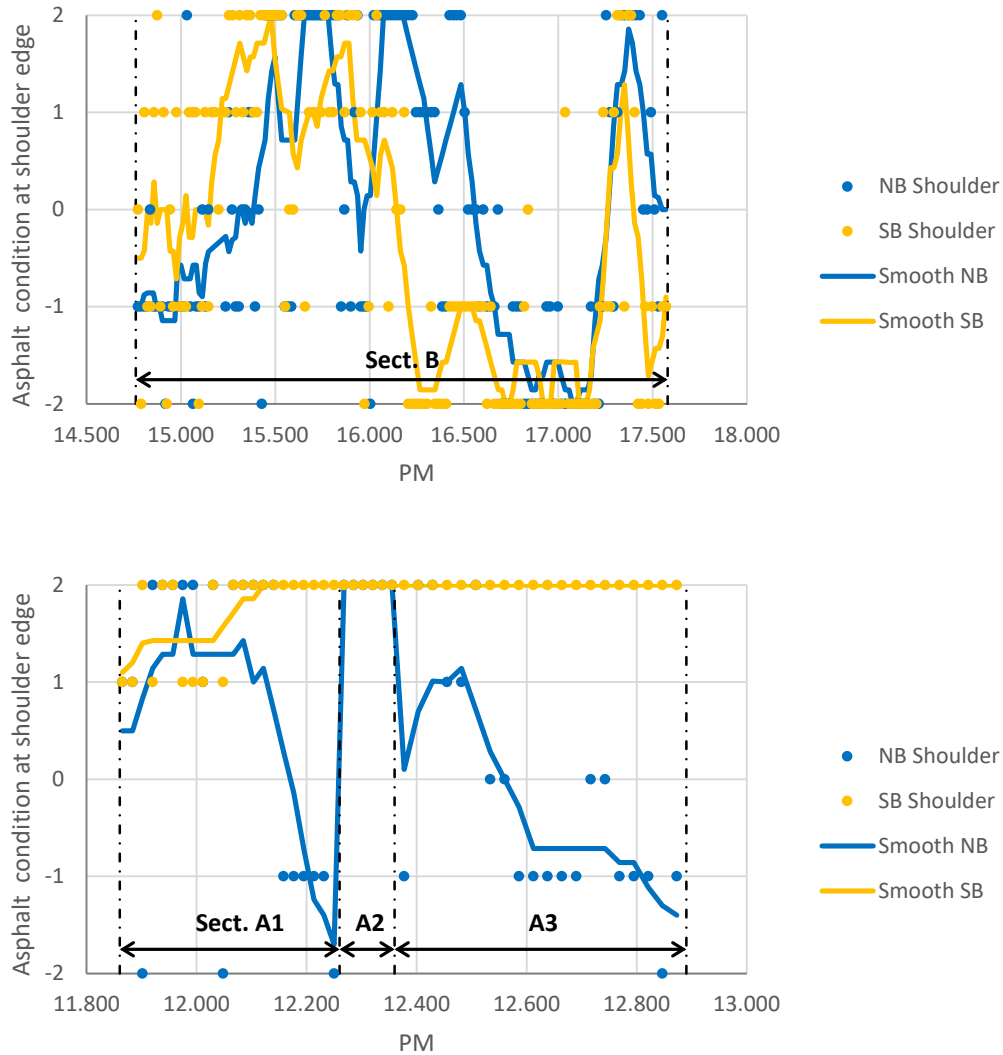


Figure 4.6: Criteria for rating asphalt condition at the shoulder edge of the roadway.

The data in Figure 4.7 indicate that the lack of asphalt base at the shoulder edge of the roadway occurs all over the project, with the exception of Segment A in the southbound direction. In Segment B, the asphalt base condition at the shoulder was especially poor. This segment's condition was attributed to (1) its original asphalt thickness only being 9 to 11 in., (2) the milling depth exceeding the 6 in. target value by 1 to 2 in., and (3) the thicker asphalt in the wheelpaths and at the center of the road than at the shoulder. As milling progressed on the overall project, the cross-slope produced by the operation occasionally exceeded the existing slope, resulting in greater milling depth at the shoulder than at the center of the roadway. This seemed to have occurred on southbound Segment B, between PM 16.000 and PM 17.580.



Note: Each point on the graphs represents the rating of a 100 ft. long roadway segment. The series “Smooth” is a moving average of the single ratings. See meaning of condition ranking (-2 to +2) in Figure 4.6.

Figure 4.7: Asphalt condition at the shoulder edge of the COA slabs.

The lack of an appropriate asphalt support at the shoulder edge of the exterior COA slabs was not the only problem. The poor condition of the milled asphalt base (as explained above) and its insufficient thickness were also problems. Based on the observation of cores and on visual inspection, it is estimated that the thickness of the asphalt remaining between the wheelpaths was between 2 and 5 in. in Segment A, and between 1 and 3 in. in Segment B. This thickness refers to the total asphalt, regardless of its condition. Nonetheless, common COA construction practice recommends a minimum of 3 in. of sound asphalt after the milling operation.

4.2 Asphalt Paving

To evaluate the use of newly placed rubberized gap-graded mix (RHMA-G) bases under COA, 0.1 mi. of SR 113 was paved with this mixture on April 25, 2019. The new asphalt was placed between PM 12.260 and PM 12.360, northbound and southbound. The old HMA was milled 1.2 in. deeper in this area than on the rest of the project to accommodate the 1.2 in. RHMA-G overlay. The RHMA-G mix had a 1/2 in. nominal maximum aggregate size and a 7.5% (by total weight of mix) asphalt rubber binder content. The asphalt rubber binder included a PG 64-10/16 base binder and an 18% crumb rubber modifier. The mix was designed, produced, and placed according to Section 39 of the 2015 Caltrans Standard Specifications. A low nominal maximum aggregate size was selected for the rubber mix so it could be placed in a thin lift. It is expected that the high binder content of the gap-graded mixes, together with the improved fatigue resistance provided by the rubber modifier, will significantly slow both the propagation of the concrete slab joints into the asphalt base and the upward propagation of any cracking in the underlying old HMA.

Pre-paving work included patching the areas with insufficient or missing asphalt base at the shoulder edge of the roadway and applying a tack coat on the milled old HMA (Figure 4.8). During the placement and compaction of the RHMA-G overlay, the air temperature was approximately 80 to 90°F, the sky was clear (Figure 4.9), and the wind speed was low (< 7 mph). The asphalt temperature during the rolling wheel compaction varied between 300°F, at the beginning of the breakdown compaction, to 200°F, at the end of the compaction process, meeting the specifications in Section 39. After the RHMA-G construction, a set of nine cores was extracted. The average air void content of the cores was 7.5% based on the saturated surface-dry method (AASHTO T 166), with individual values varying from 4% to 10%. This variation percentage is relatively high, but it is similar to the variation observed in the same asphalt mix type in overlays with similar thicknesses. The upper limit of the variation range was slightly above the 9% maximum prescribed in Section 39. The larger the air void content of the asphalt mix, the lower the stiffness and the greater the moisture susceptibility will be. The RHMA-G thickness varied from 1.2 to 1.8 in., with an average value of 1.5 in.

It should be noted that all the cores extracted from the newly placed RHMA-G showed debonding between the asphalt lifts. The total thickness was extracted in two pieces: (1) the top piece, which was 2.5 in. thick on average, included the newly placed RHMA-G plus bonded old HMA and (2) the bottom piece, which was 2.3 in. thick on average, included the debonded part of the old HMA (see examples in Figure 4.10).



Patching areas with insufficient or missing asphalt base at the shoulder edge of the roadway



Tack coat application

Figure 4.8: Preparations for asphalt paving.



Figure 4.9: Asphalt placement and compaction.



Note: The top pieces of the cores (on the left in each picture) included the newly placed RHMA-G plus the bonded old HMA; the bottom pieces included the debonded part of the old HMA.

Figure 4.10: Examples of cores extracted from the newly placed RHMA-G.

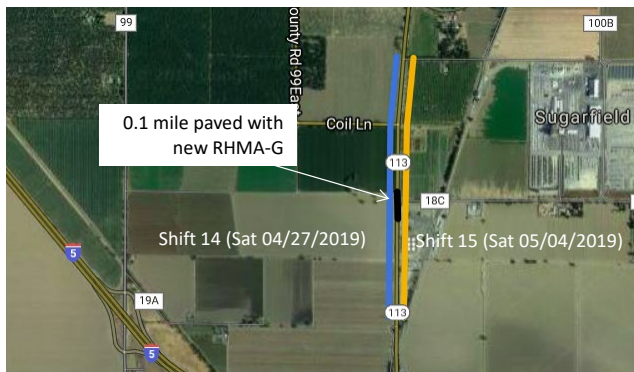
4.3 Construction of the Overlay

4.3.1 Construction Timing

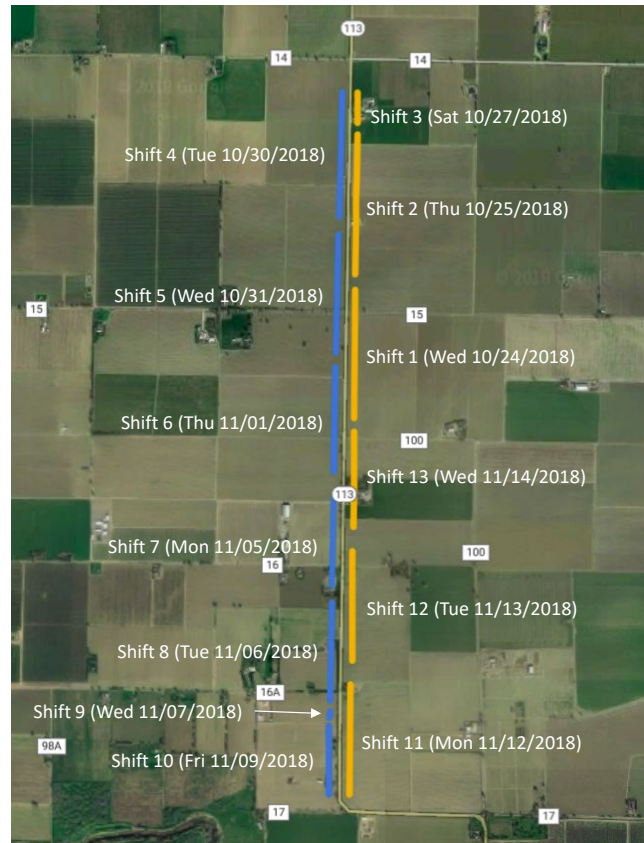
The concrete was mixed at the Elite Ready Mix Rio Linda plant in Pleasant Grove, California, 25 miles from the SR 113 construction site. The concrete overlay was placed in 15 paving shifts. Segment B was paved between October 24 and November 9, 2018. During weekdays, the Segment B concrete paving operations took place at night to prevent traffic congestion. The Segment A paving operations took place during the day on two Saturdays, April 27 and May 4, 2019. The layout of each paving shift is shown in Figure 4.11 and Table 4.1.

4.3.2 Preparatory Work

Preparing the asphalt surface for construction of the overlay included these steps: patching the asphalt where the milled asphalt base had been removed or was insufficient (Figure 4.5), placing the tie bar baskets, and moisture conditioning the asphalt surface. Despite a prescription in the project special provisions calling for a thorough asphalt surface cleaning before placement of the concrete overlay, this task was not performed. Instead, an asphalt surface cleaning operation was only performed after the milling was completed. Further, this cleaning operation did not include an air pressure cleaning that would normally ensure the removal of dust, grit, and foreign material. Similarly, the newly placed RHMA-G was not cleaned to eliminate surface contamination before placement of the concrete overlay. As a result, the asphalt surface was not as clean as is desired for COA construction (Figure 4.12), and this may have had a negative effect on the concrete-asphalt bonding.



Segment A



Segment B

Note: For the Segment B nighttime paving shifts, the date in the picture is the day paving began (at night). For example, Shift 1 paving took place between the evening of October 24 and the early morning of October 25.

Figure 4.11: Concrete paving shifts.

Table 4.1: Concrete Paving Shifts

Paving Shift	PM Start	PM End	Direction	Length (mi.)
Shift 1	16.237	16.791	North	0.554
Shift 2	16.791	17.412	North	0.621
Shift 3	17.412	17.580	North	0.168
Shift 4	17.580	17.017	South	0.563
Shift 5	17.017	16.479	South	0.538
Shift 6	16.479	15.997	South	0.482
Shift 7	15.997	15.549	South	0.448
Shift 8	15.549	15.092	South	0.457
Shift 9*	15.092	15.065	South	0.027
Shift 10	15.065	14.764	South	0.301
Shift 11	14.764	15.228	North	0.464
Shift 12	15.228	15.772	North	0.544
Shift 13	15.772	16.237	North	0.465
Shift 14	12.886	11.856	South	1.030
Shift 15	11.856	12.886	North	1.030

* Paving halted because of a problem with the mixing plant.



Note: Dirt on the asphalt surface has a negative impact on concrete-asphalt bonding.

Figure 4.12: Dirt on the asphalt surface before concrete paving.

Tie bar baskets were used for the midlane longitudinal joint, as shown in Figure 4.13, except for a small portion in the northbound lane around PM 12.655, where a noncompliant handmade system was used. The tie bars of the longitudinal joint between lanes were inserted manually into the plastic concrete, as shown in Figure 4.14. This technique, which is not one of the options prescribed in Caltrans Standard Specifications, Section 40 yields little control of the tie bar position and allows air pockets to form in the concrete around the manually inserted tie bar.



Compliant tie bar baskets



Handmade system used on a small portion of the project, northbound lane around PM 12.655

Figure 4.13: Tie bar baskets fastened to the asphalt base.



Manual insertion of tie bars in the plastic concrete



Air pocket around the manually inserted tie bar

Note: Manual insertion of the tie bars in the plastic concrete is not one of the options prescribed in Caltrans Standard Specifications, Section 40.

Figure 4.14: Manual insertion of tie bars in the plastic concrete.

Before placement of the concrete overlay, the asphalt surface was wet conditioned by a truck that sprayed water on it. Overall, the asphalt surface was adequately wet conditioned; it was wet but free of standing water, approximating a saturated surface-dry condition (Figure 4.15, left). At some spots, however, the asphalt surface dried before the concrete was placed (Figure 4.15, right) and it would have been beneficial to have sprayed these spots with water manually. At other locations, the irregularity of the milled asphalt surface caused water ponds to form at the shoulder edge of the roadway (Figure 4.15, right). This standing water may have had a negative effect on the concrete poured at these locations.



Asphalt surface is adequately wet conditioned: uniformly moist but free of standing or flowing water



Asphalt surface is not adequately wet conditioned: some dry areas; standing water at the shoulder

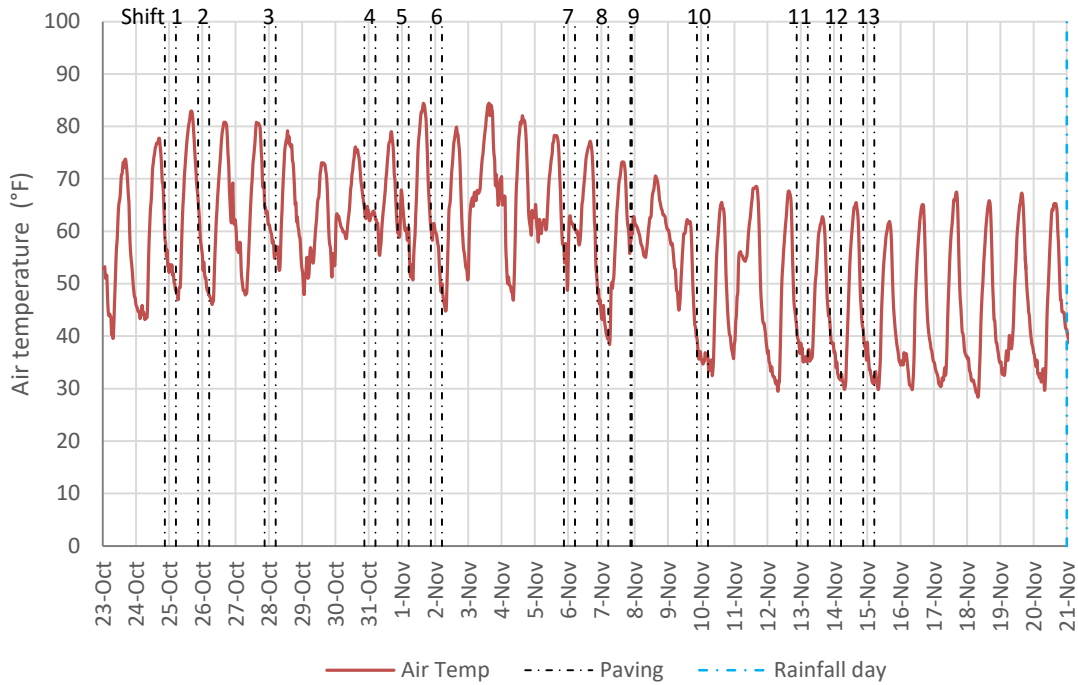
Figure 4.15: Asphalt surface moisture conditioning.

4.3.3 Construction Weather Conditions

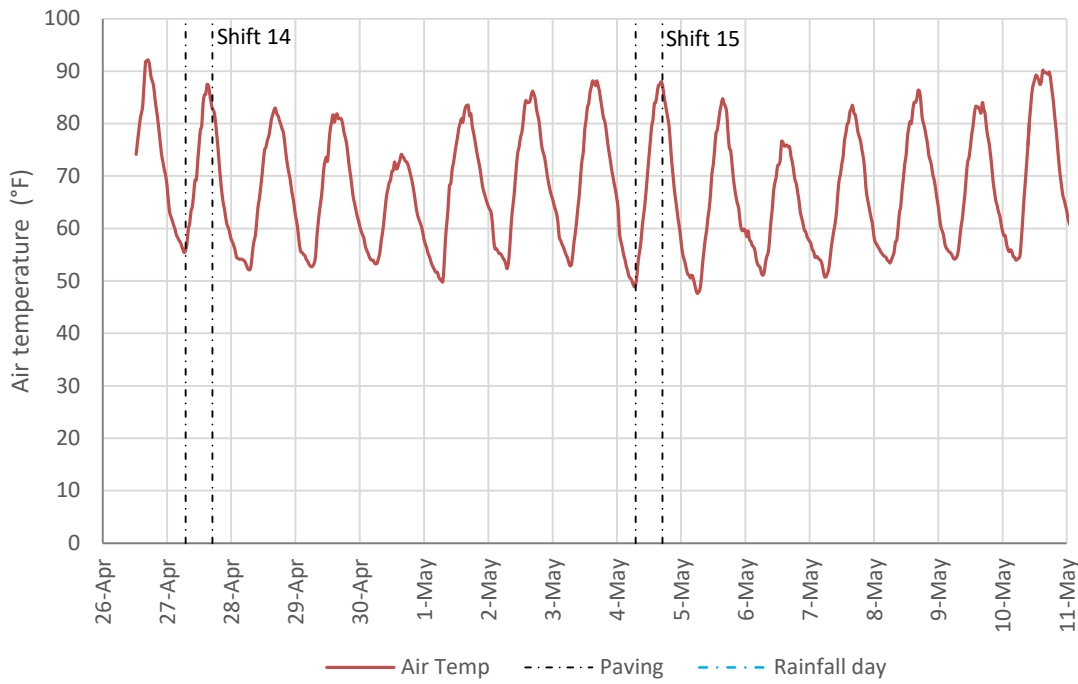
Weather conditions were monitored by a weather station at the Caltrans Woodland District 3 maintenance center, which is located about half a mile south of the COA project. Since that weather station was located near a building that might have interfered with wind monitoring, the wind speed reported by the website Time and Date AS (www.timeanddate.com) was used instead. Figure 4.16 shows the air temperatures and time window for each of the 15 paving shifts. The maximum and minimum air temperatures during each paving shift are shown in Figure 4.17. Overall, air temperatures were low during the Segment B paving due to the time of the year (October and November) and the nighttime operations. Temperatures were particularly low during paving Shifts 10 through 13, with the lowest values in the 30s and low 40s Fahrenheit.

Caltrans Standard Specifications do not dictate an air temperature range for concrete paving. Instead, the specifications require that (1) immediately before the concrete is placed, the temperature of the mixed concrete must fall between 50 to 90°F and (2) the concrete pavement surface temperature must be maintained at not less than 40°F for the initial 72 hours. (The fulfillment of these two requirements is evaluated in the next section of the report.)

Wind speed was particularly high during paving Shifts 4, 7, and 9, when it reached its maximum values of 10 to 15 mph (Figure 4.18).



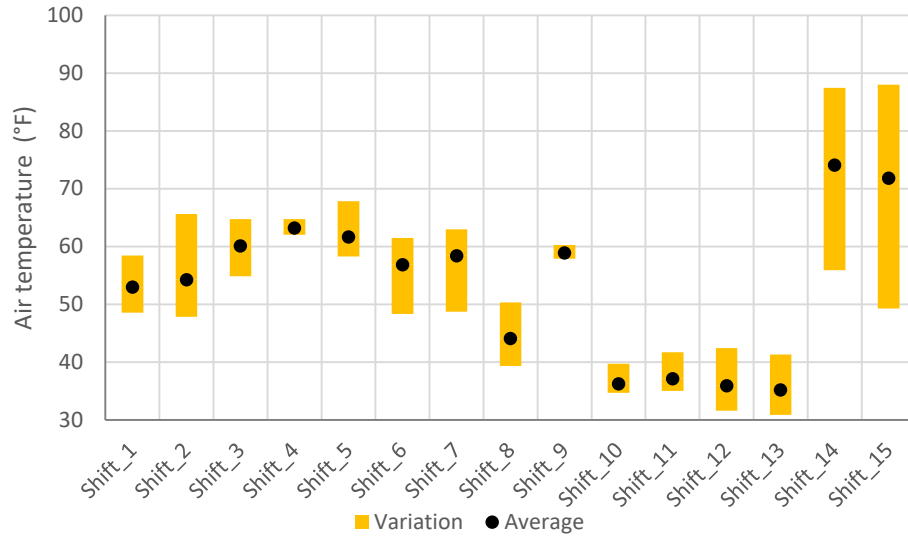
Segment B paving, October 24 to November 14, 2018



Segment A paving, April 27 and May 4, 2019

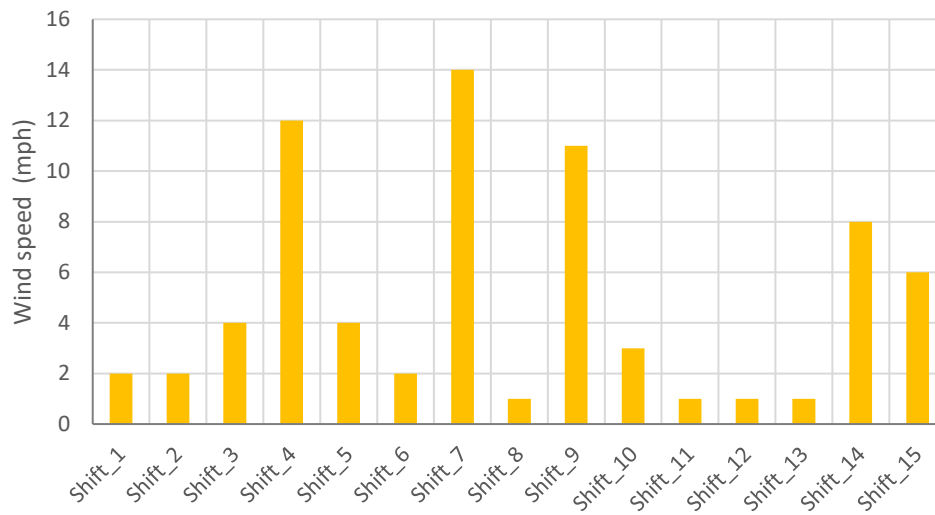
Note: See Figure 4.11 for the layout of each of the 15 paving shifts.

Figure 4.16: Air temperatures during concrete paving.



Note: See Figure 4.11 for the layout of each of the 15 paving shifts.

Figure 4.17: Air temperature variations during concrete paving.



Note: See Figure 4.11 for the layout of each of the 15 paving shifts.

Figure 4.18: Maximum wind speeds during concrete paving.

4.3.4 Concrete Paving

The concrete was transported in ready-mix trucks about 25 miles from the plant to the construction site. A full road closure was approved by Caltrans, allowing the lane that was not being paved to provide the ready-mix trucks access to the paving front (Figure 4.19). A side-belt spreader was used to pour the concrete onto the lane being paved and to spread it across the width for paving. The slipform paver was a Gomaco Commander III (Figure 4.20).



The ready-mix trucks discharge concrete on the belt, then the belt pours the concrete onto the lane. Finally, the spreader spreads the concrete over the width of the lane.



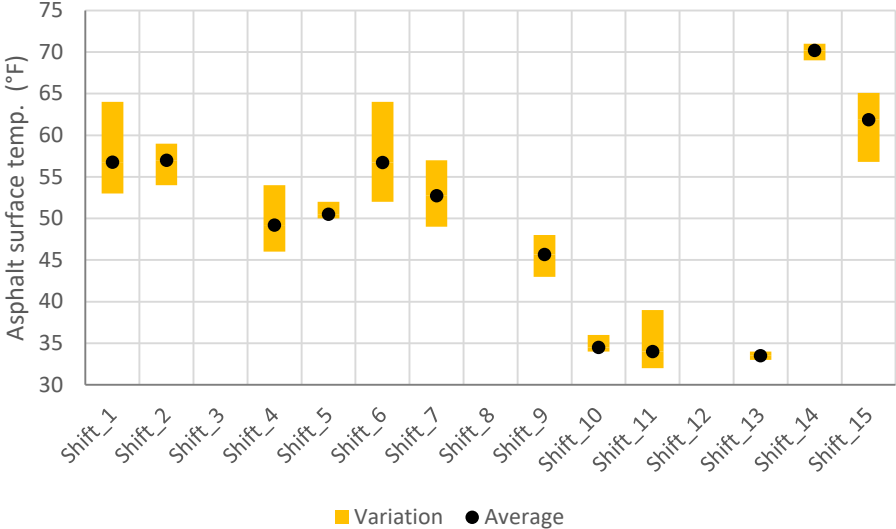
Occasionally, the ready-mix trucks discharged concrete directly on the lane, then the spreader spread the concrete over the width of the lane.

Figure 4.19: Concrete pouring.



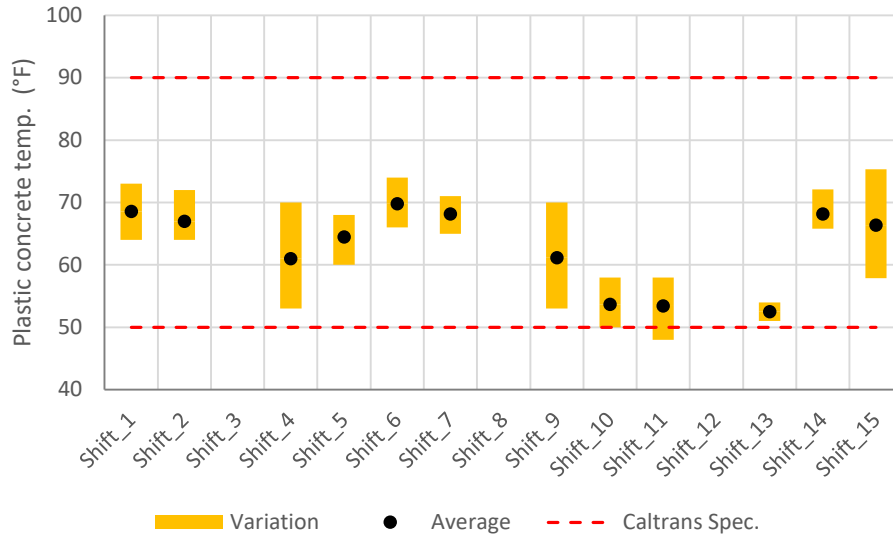
Figure 4.20: Slipform paver.

During the concrete paving, the asphalt surface temperature ranged from the low 30s to the low 70s Fahrenheit (Figure 4.21). The asphalt surface temperatures were much lower than the 120°F limit prescribed by the project special provisions. The asphalt surface temperature was particularly low during paving Shifts 10 through 13, due to the low air temperatures on those days and during the nighttime paving. Even though neither the Caltrans Standard Specifications nor the project special provisions prescribed a minimum asphalt surface temperature during concrete paving, it would still have been desirable for the temperature to not drop below 50°F. This 50°F minimum agrees with the Caltrans Standard Specifications, Section 90 requirement that “immediately before placing the concrete, the temperature of the mixed concrete must be from 50 to 90°F.” The temperature of the plastic concrete was also measured during the construction of the overlay, with the results shown in Figure 4.22. Some measurements were below 50°F, but these were taken between the side-belt spreader and the paver, not immediately before placing the concrete.



Note: See Figure 4.11 for the layout of each of the 15 paving shifts. Temperature was measured with temperature guns.

Figure 4.21: Asphalt surface temperature variation during concrete paving.

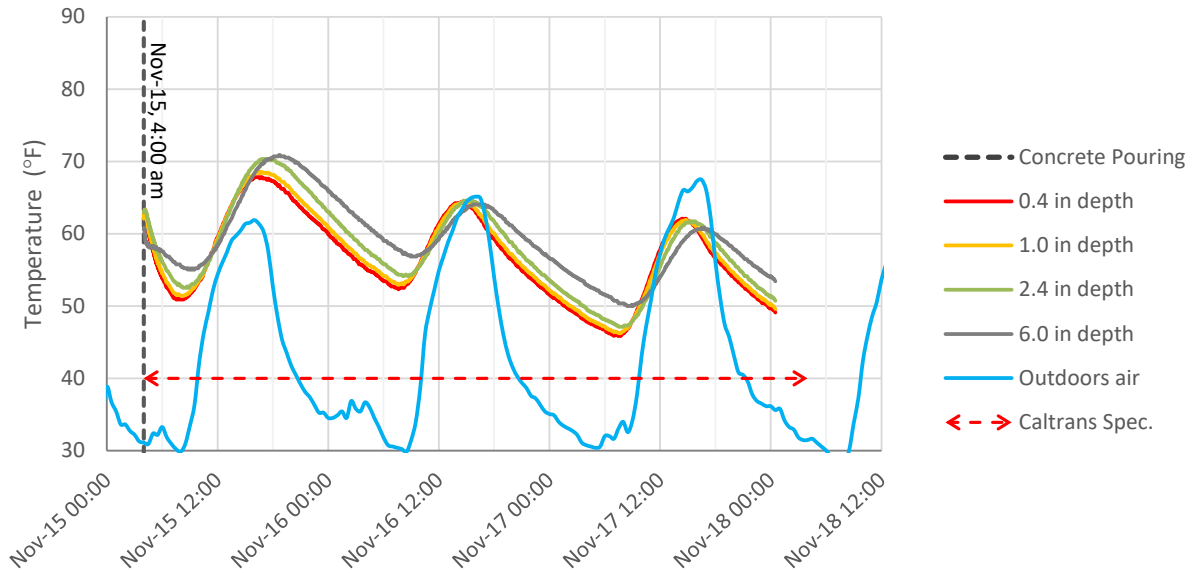


Note: See Figure 4.11 for the layout of each of the 15 paving shifts. Temperature was measured with temperature guns at the truck discharge chute, in front of the side-belt spreader, and between the spreader and the paver.

Figure 4.22: Plastic concrete temperature variation during concrete paving.

Caltrans Standard Specifications, Sections 40 and 90 require that concrete remain at a minimum temperature of 40°F during the initial 72 hours after paving. To verify the fulfillment of this prescription, the temperature was monitored at different depths in the concrete overlay during and after one of the coldest paving shifts (November 14, at night). As shown in Figure 4.23, the concrete temperature remained above 40°F during the first 72 hours despite air temperatures having dropped to the freezing point.

Some of the transverse construction joints (beginning/end on paving shifts) were built incorrectly. Specifically, at the first construction joint (Section B, northbound direction, between paving Shifts 1 and 2), tie bars rather than dowels had been installed (Figure 4.24). After learning of the issue, the resident engineer instructed the contractor to use dowels at the transverse construction joints. Even though this was done, in some cases lubricant was applied either poorly or not at all. As a result, some of these joints may have locked.



Note: Concrete temperature was measured at different depths in the slab by means of a thermocouple rod. The paving reached the thermocouple rod at 4:00 a.m., November 15.

Figure 4.23: Concrete temperature monitoring, paving Shift 13 (November 14, at night).



Figure 4.24: Installation of tie bars instead of dowels at a transverse joint (end of paving Shift 1).

4.3.5 Concrete Finishing

The concrete surface was finished with bull floats and edge trowels, and then longitudinal tining was applied by hand-pulling a metal rake along the surface to create grooves in the pavement with a depth of approximately 3/16 in. Both operations were conducted immediately after the paver passed, while the concrete was still workable (Figure 4.25).



Bull float finishing



Metal-rake tining

Figure 4.25: Surface-finishing and tining.

A few localized surface imperfections were detected about two weeks after construction of the Segment B overlay. They were most likely due to contamination of the concrete during placement and finishing.

4.3.6 Concrete Curing

The concrete overlay was cured with a curing compound that meets ASTM C309 Type 2 (white pigmented), Class B (resin based) specifications. The compound was applied manually (Figure 4.26) at a nominal rate of 150 ft²/gal.



Manual spraying of curing compound



Appearance of the final surface

Figure 4.26: Curing compound application.

Section A22 was cured with an SRA solution before the standard curing compound was applied. The timing and concentration of the SRA solution application depend on the properties of the concrete, weather conditions, and target dosage. Three applications of the solution at 50% concentration were required to supply the target SRA dosage (8.5 oz./yd²). The SRA solution was applied in stages to ensure that the concrete fully absorbed all of it. If the solution is applied faster than the concrete can absorb it, there is a risk that the water will evaporate before the SRA penetrates into the concrete pores, leaving it on the surface. The first SRA spray was applied after the concrete surface's sheen disappeared and it looked dry, as shown in Figure 4.27 (left). The rest of the SRA solution was applied after the concrete had adsorbed the solution applied previously. The timing and dosage of the three applications are presented in Table 4.2. The final applied dosage was 8.8 oz. SRA/yd². As shown in Figure 4.27 (right), the SRA solution was applied manually.



Surface appearance before SRA application



Manual application of the diluted SRA

Note: Section A22 was only 42 ft. long (seven slab lengths); it was located at PM 12.360 in the northbound lane.

Figure 4.27: Application of the shrinkage-reducing admixture on Section A22.

Table 4.2: SRA Application on Section A22

	Start	End	Amount of SRA Solution
Section A22 paving	8:32 am	8:42 am	
1st SRA application	10:20 am	10:24 am	3 gal.
2nd SRA application	11:33 am	11:37 am	3 gal.
3rd SRA application	11:47 am	11:52 am	3 gal.
Total solution (50% SRA)			9 gal.
Total SRA			4.5 gal.
SRA dosage (588 ft ²)			8.8 oz. SRA/yd ²
Curing compound*	12:20 pm	12:22 pm	

* Standard curing compound was sprayed on Section A22 after SRA application.

The topical use of SRA was tried for the first time in a full-scale experiment in the 4.58B research project (6), and there the concrete seemed to absorb the SRA solution much faster than in the Woodland SR 113 overlay. This outcome is believed to be due to differences between the projects' concrete mixtures. More specifically, the outcome is believed to be related to differences between the mixtures' ratio of water to total cementitious materials (w/cm) and the speed of cement hydration. The mixture treated with SRA in the 4.58B research project, which was designed to be opened to traffic in 10 hours, had a low w/cm ratio, 0.33, and used a large dose of accelerator. Consequently, internal desiccation was expected shortly after concrete placement. It is believed that the early internal desiccation helped the concrete to absorb the SRA solution in the 4.58B research project.

4.3.7 Joint Saw-Cutting

Joints were cut to a depth of one-third of the slab thickness, which resulted in 2 in. saw cuts (Figure 4.28). The cutting operation was conducted between six and eight hours after the concrete was placed. No early-age cracking was observed. If any random cracks were noticed, they would likely be due to late sawcutting.



Figure 4.28: Sawcutting operation.

4.3.8 Opening to Traffic

A granular backfilling operation was conducted outside the concrete shoulder before the road was opened to traffic (Figure 4.29). Segment B was opened to traffic on November 18, 2018, three days after the Segment B concrete overlay paving concluded. Segment A was opened to traffic on May 10, 2019, six days after the concrete overlay paving concluded.



Figure 4.29: Shoulder backfilling.

4.3.9 *Diamond Grinding*

The postconstruction longitudinal smoothness of the concrete overlay was relatively poor, as shown by the Pre-G (pre-grinding—i.e., before grinding) series in Figure 4.30 and Figure 4.31. The 0.1 mi. mean roughness index (MRI) varied from 70 to 175 in./mi., which was considerably higher than the 60 in./mi. upper limit prescribed by Section 40 of the 2015 Caltrans Standards Specifications that apply to this project. The MRI limits series in Figure 4.30 and Figure 4.31 are based on the 2019 Caltrans smoothness specifications, Table 67.5 (JPCP reconstruction). This table includes payment disincentives for MRIs between 75 and 90 and mandatory grinding when MRI exceeds 90 in./mi. Even though these specifications are not applicable to this project, an evaluation of the concrete overlay pre- and post-grinding smoothness followed by a comparison of those against the new Caltrans specifications was regarded as an interesting exercise. It revealed that the entire project would have required mandatory grinding since the MRI exceeded 90 in./mi at all the 0.1 mi. segments.

The cause of the Pre-G MRI being so high is unclear. The information collected for the overlay construction evaluation was insufficient to establish a sure explanation for the high postconstruction MRI, and finding the explanation would require an extensive monitoring program because concrete pavement smoothness is the result of a complex process that involves many factors (7). Evaluating each one's effect on smoothness far exceeds the scope of this project. The MRI values on Segments A and B were especially high considering that the segments are essentially flat, straight lines. Typically, changes in superelevation and vertical slope are likely to have a negative impact on smoothness. Here, the absence of curves on the segments eliminated the need to set a corresponding superelevation, and their flat layout eliminated the need to change the road's vertical slope. The paver was able to operate with almost no interruptions since the trucks had relatively easy access to the construction site and, overall, their arrival was steady. Further, the segments should have been smoother because there were no bridges, intersections, or other elements to interrupt the paving operation. Another factor that should

have contributed to a smooth pavement was the use of a side-belt spreader, which helps maintain the stability of the concrete head in the paver box (constant level of fresh concrete in front of the paver), and that stability has been shown to improve smoothness (7). Finally, no considerable changes in fresh concrete consistency were observed.

Several factors are believed to have impacted smoothness negatively:

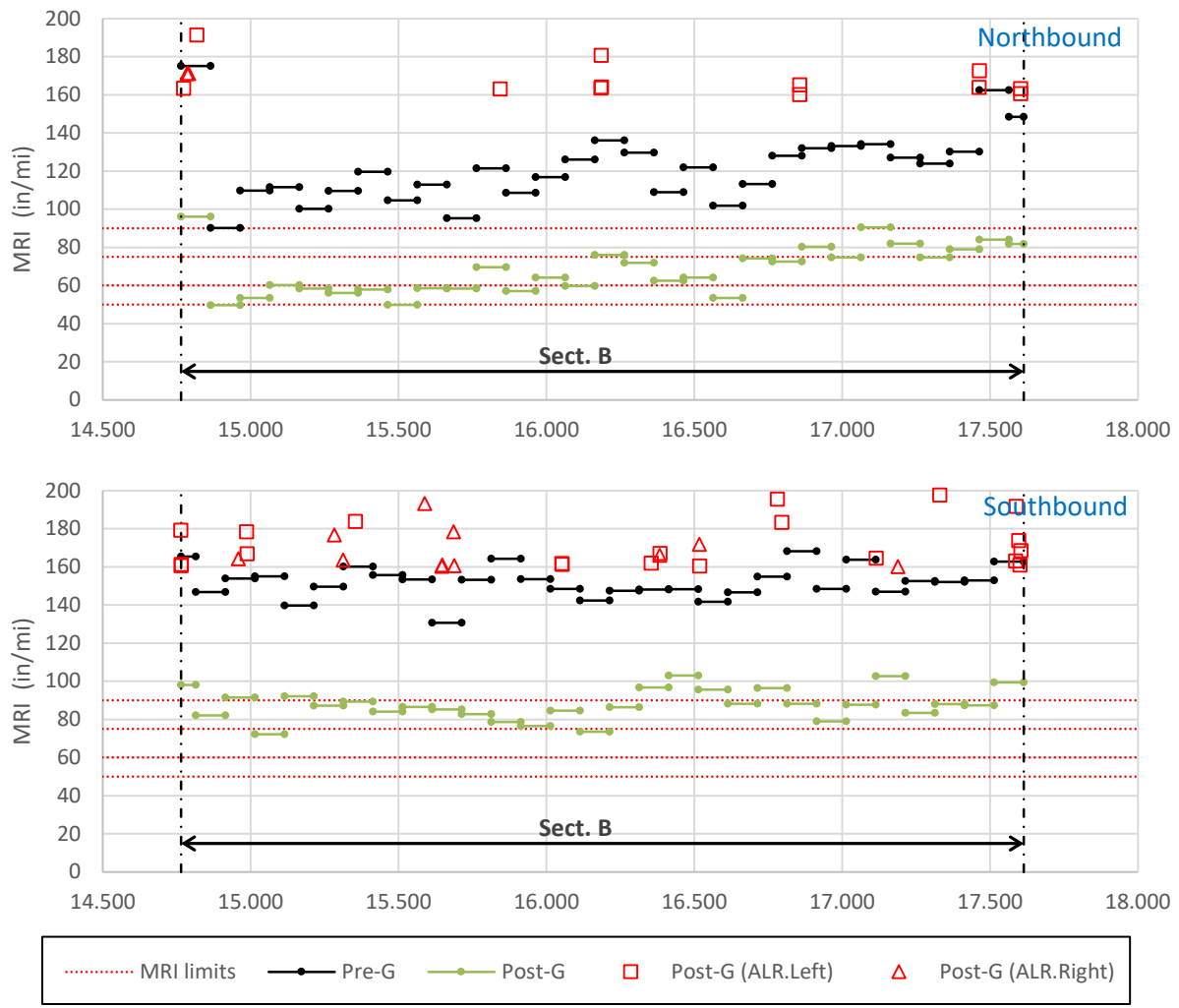
- The milled asphalt surface was very uneven, which resulted in poor slab thickness uniformity and, consequently, in difficulties maintaining a stable concrete head.
- The exterior paver track, the soil outside the paved lane, was very uneven since it lay outside the shoulder. Most of the unevenness of this track is compensated by the paver hydraulic system, but some of it may still show on the overlay surface.
- The correct alignment of the string line was not verified.
- Gaps between 2 and 23 days elapsed between the overlay construction and the initial MRI evaluation on the segments. During these periods, slab warping due to the onset of differential drying shrinkage and slab curling due to temperature gradients within the slabs produced a negative impact on the smoothness of the overlay. This impact could be quantified in Segment A because the curvature of the slabs was measured with VWSGs. An estimate based on slab curvature measurements and *ProVAL* calculations indicated that between 20 and 25 in./mi. of the initial MRI were caused by the slab drying shrinkage and temperature gradients.

Regardless of which factor or factors affected the overlay smoothness, the large MRI values measured emphasize the need to explore use of modern techniques like stringless (3D) paving and real-time smoothness evaluation to achieve smoother concrete surfaces. After all, road surface smoothness is the functional variable with the largest impact on ride quality.

To try to meet Caltrans smoothness specifications, the complete project was subjected to grinding (blanket grinding). The appearance of the post-grinding surface can be seen in Figure 4.32. Grinding operations took place in April 2019 on Segment B and in the second half of May 2019 on Segment A. Overall, the grinding resulted in a 40% MRI improvement, although the improvement for individual 0.1 mi. segments varied from 19% to 53% (Figure 4.33).

Based on the Post-G (post-grinding) series results shown in Figure 4.30 and Figure 4.31, few of the 0.1 mi. segments (around 14% of the project length) passed the 60 in./mi. requirement, but most of them (around 82% of the project length) would have passed the 90 in./mi. requirement.

Figure 4.30 and Figure 4.31 also show the areas of localized roughness present after the grinding operation; the roughness of these areas was categorized according to the 2019 Caltrans smoothness specifications (160 in./mi. limit). As shown in the figures, a considerable number of areas of localized roughness (ALRs) still existed after the grinding operation.



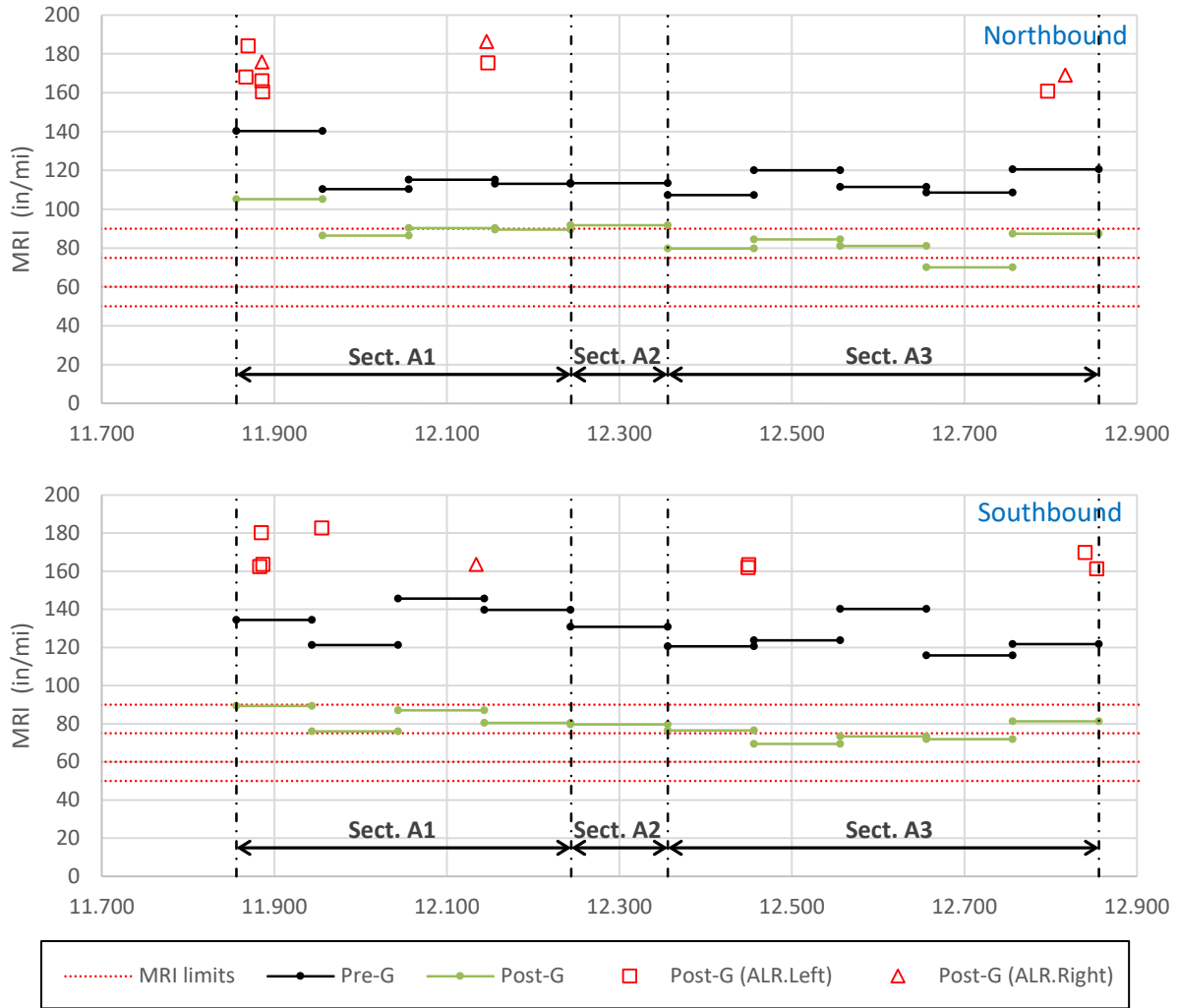
Notes: The mean roughness index limits were based on the 2019 Caltrans smoothness specifications, Table 67.5. These specifications were not applicable to the Woodland SR 113 COA.

Pre-G = pre-grinding (before grinding of the overlay), Post-G = post-grinding (after grinding of the overlay).

MRI is the average of the IRI values for the left and right wheelpaths using a 0.1 mi fixed interval and a 250 mm filter, determined with *ProVAL*.

Area of localized roughness is an area where IRI exceeded 160 in./mi. The IRI was determined as the moving average of the IRI values for each wheelpath using a 25 ft. continuous interval and a 250 mm filter, determined with *ProVAL*.

Figure 4.30: Longitudinal smoothness: Segment B.



Note: The mean roughness index limits were based on the 2019 Caltrans smoothness specifications, Table 67.5. These specifications were not applicable to the Woodland SR 113 COA.

MRI is the average of the IRI values for the left and right wheelpaths, using a 0.1 mi. fixed interval and a 250 mm filter, determined with *ProVAL*.

Pre-G = pre-grinding (before grinding of the overlay), Post-G = post-grinding (after grinding of the overlay).

Area of localized roughness is an area where IRI exceeded 160 in./mi. The IRI was determined as the moving average of the IRI values for each wheel path using a 25 ft. continuous interval and a 250 mm filter, determined with *ProVAL*.

Figure 4.31: Longitudinal smoothness: Segment A.



Concrete surface grinding



Area on the left side of the photo has been ground; area on the right has not been ground yet (and retains its tined texture)

Figure 4.32: Diamond grinding.

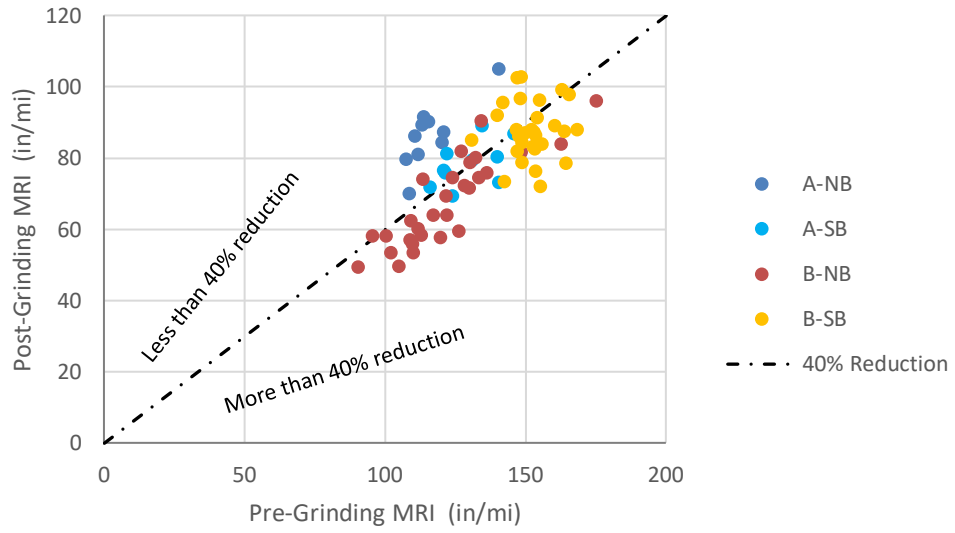


Figure 4.33: MRI improvement due to grinding.

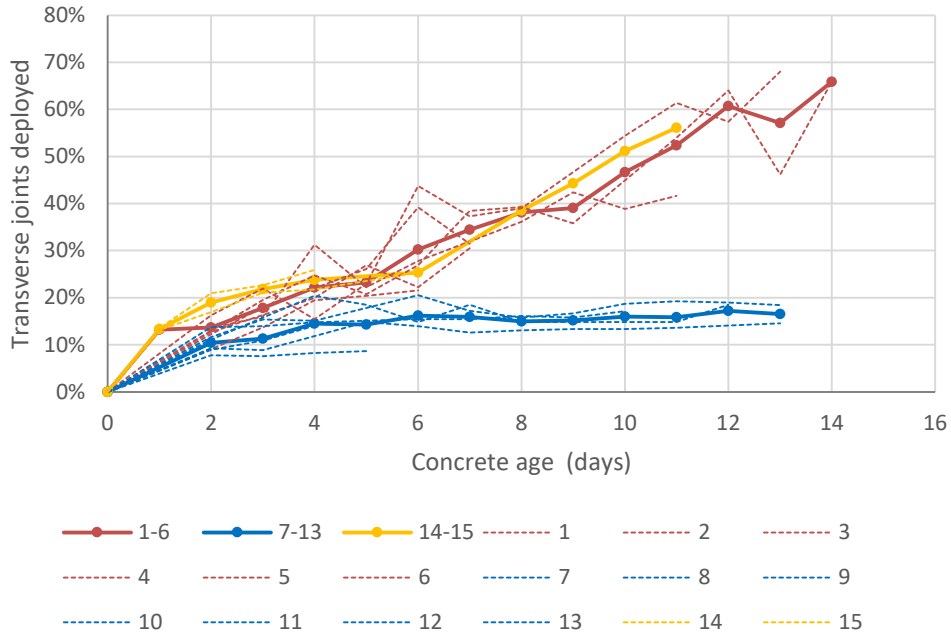
4.3.10 Transverse Joint Deployment

Deployment of the transverse joints was evaluated visually, by examining the edges of the concrete overlay (Figure 4.34). The joint deployment evaluation started the day after the concrete overlay construction and continued every day until the edges of the overlay were no longer visible. (Note: a granular backfill was built outside the concrete shoulder before the road was opened to traffic; this backfill covered the edge of the concrete overlay, making the edge of the transverse joints invisible.)



Figure 4.34: Deployed transverse joints.

The percentage of deployed transverse joints is shown in Figure 4.35. At first the transverse joints deployed over relatively long time intervals: roughly one out of every six to ten transverse joints deployed within one to two days after the overlay construction (as shown in Figure 4.35). That represents a cracking spacing of 35 to 60 ft., which is in the lower range of the values reported for regular jointed plain concrete pavements in the literature (8). This initial cracking was mainly driven by the thermal contraction of the concrete after setting. The next transverse joint deployments were mainly driven by the concrete drying from the top down. The joint deployment increased rapidly for most of the paving shifts until it reached about 60% after two weeks. This outcome agreed with the results from Project 4.58B, where 100% of the transverse joints deployed (9). It has been reported that in wet US states not all the transverse joints of 6 ft. long slabs get to deploy. The transverse joint deployment was very slow for paving Shifts 7 through 13 because the cloudy weather after the construction slowed the drying of the concrete overlay surface.

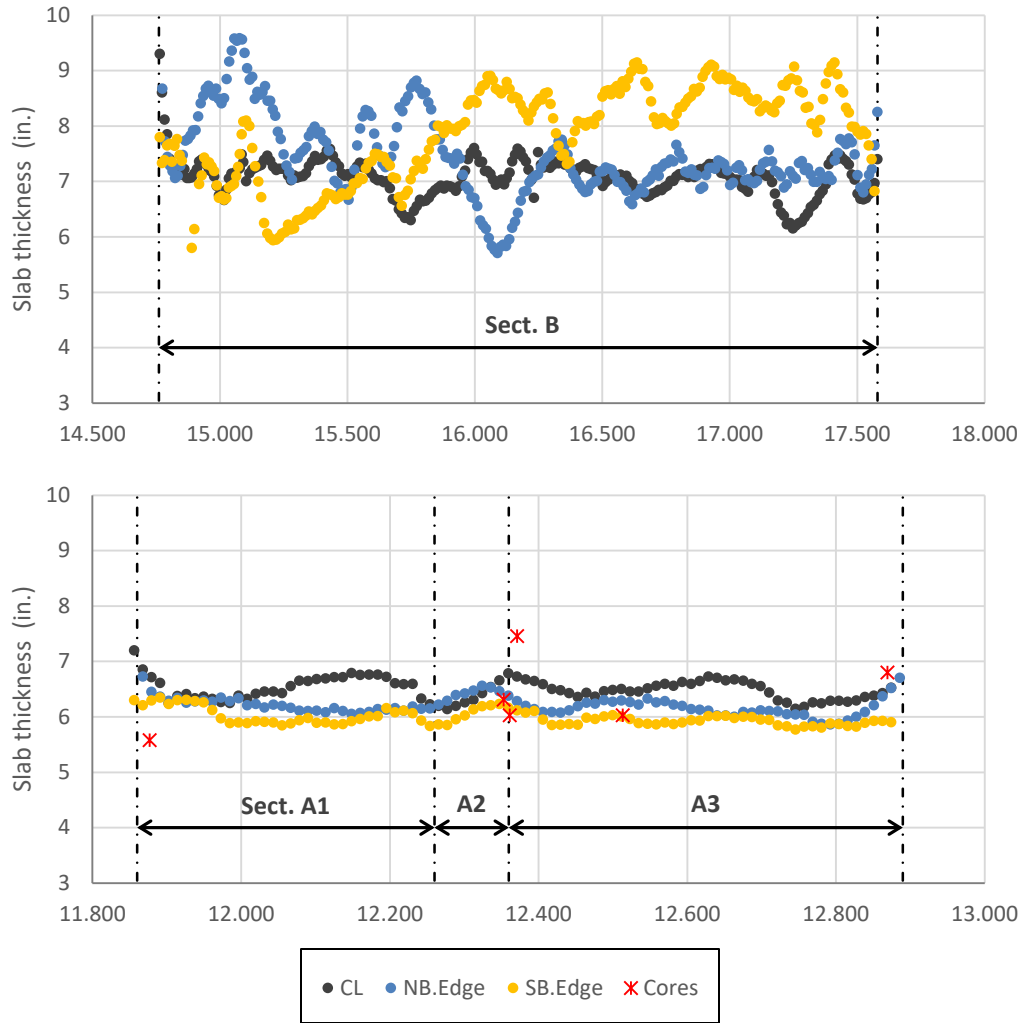


Note: The series number corresponds to the paving shift.

Figure 4.35: Evolution of transverse joint deployment.

4.3.11 Concrete Overlay Thickness

Slab thickness was measured manually after the concrete overlay placement, with one record taken every 10 slabs. The results are presented in Figure 4.36. As shown in this figure, the concrete overlay in Segment B was 1 to 3 in. thicker than the 6 in. target. The measurements were taken before the blanket grinding was applied, so concrete overlay thickness could be 1/6 to 1/4 in. thinner than the values shown in Figure 4.36.



Note: Slab thickness was measured manually, every 10 slabs, right after the overlay placement (before grinding).

CL is centerline, NB is northbound, SB is southbound.

The cores were extracted 3 ft. from the centerline after grinding (grinding may remove 1/6 to 1/4 in.).

Figure 4.36: Slab thickness.

5 LABORATORY TESTING OF CONCRETE MECHANICAL PROPERTIES

The concrete overlay mixture was sampled on four occasions and used to prepare field specimens that would be later tested in the laboratory. The four sets of samples—referred to as Trial Slabs, Field0, Field1, and Field2 in this report—are described below:

- Trial Slabs (09/18/2018 12:00 pm). A set of trial slabs was built at the UC Davis facility of the UCPRC on September 18, 2018. The set was built to test the procedure for installing the different sensors in the concrete. The concrete mixture was produced by the same plant that made it for the final construction of the Woodland SR 113 overlay.
- Field0 (10/30/2018 11:00 pm, Segment B). This set of beams was prepared to test whether the cold air temperatures during the paving of Section B had a negative impact on concrete flexural strength.
- Field1 (11/02/2018 12:40 am, Segment B). This set of specimens was to be subjected to a comprehensive mechanical characterization (strength, stiffness, coefficient of thermal expansion [CTE], and shrinkage).
- Field2 (05/04/2019 11:20 am, Segment A). This set of specimens was to be subjected to a comprehensive mechanical characterization (strength, stiffness, CTE, and shrinkage).

Except for the drying shrinkage test, all the specimens were prepared and tested following ASTM standards. Three specimens per test and per testing age were used. Although ASTM C157-17 specifies that the drying shrinkage test specimens remain in water storage until the concrete reaches an age of 28 days, the specimens in this project were demolded after 24 hours and only stored in water until the concrete reached an age of 4 days. This procedure is close to the Section 90 of the Caltrans Standards Specifications, which require storing the specimens in water until the concrete reaches an age of 7 days.

The concrete flexural strength results are presented in Figure 5.1. Because the mixture was designed to be opened to traffic after 24 hours, it easily met Caltrans 28-day flexural strength requirement of 570 psi (note: there were some differences between the curing procedure followed in this research project and the one specified in Caltrans Test 523). The compressive strength and modulus of elasticity results are shown in Figure 5.2 and Figure 5.3, respectively. These results will be used with the flexural strength results in the mechanistic analysis of the pavement.

The concrete's CTE was around $5.2 \mu\epsilon/^\circ\text{F}$ (Figure 5.4). This CTE value is within the typical range that can be expected for pavement concrete in California. A petrographic analysis of the concrete's coarse aggregate was unavailable.

The drying shrinkage results are shown in Figure 5.5. The measured drying shrinkage was relatively high, particularly compared to the limit of 500 $\mu\epsilon$ after 28 days drying that is prescribed by Caltrans Standard Specifications, Section 90. Field1 prisms reached 650 $\mu\epsilon$ shrinkage after 28 days while the Field2 prisms reached 800 $\mu\epsilon$ at that same age. Nonetheless, these values cannot be directly compared to the Section 90 500 $\mu\epsilon$ limit for two reasons. First, the moisture-curing period prescribed in Section 90 lasts until the specimens are seven days old, which is longer than the moisture-curing applied to the specimens in this research project. And second, the Section 90 limit refers to laboratory specimens, but the specimens used in this project were sampled and prepared in the field. According to ASTM C157-17 (note 2), field specimens “can show up to twice as much drying shrinkage as laboratory cast specimens from the same materials and proportions.”

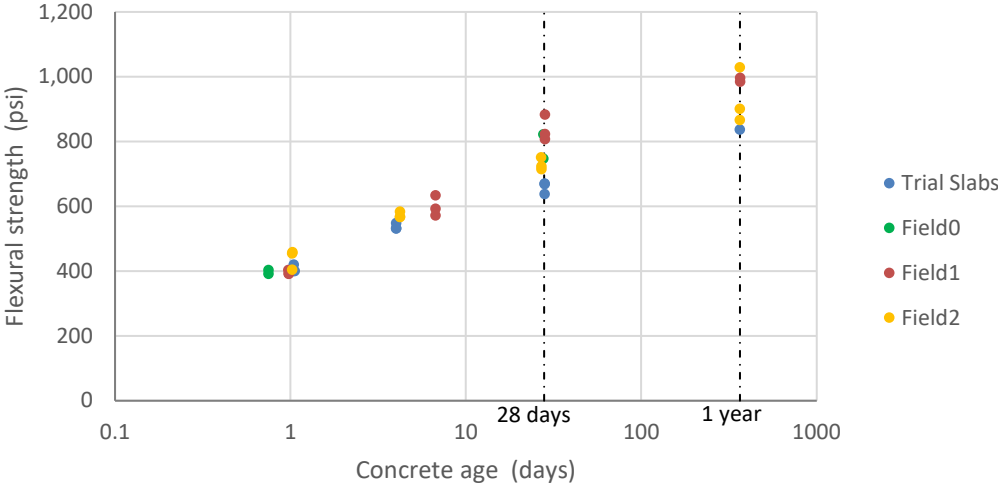


Figure 5.1: Concrete flexural strength.

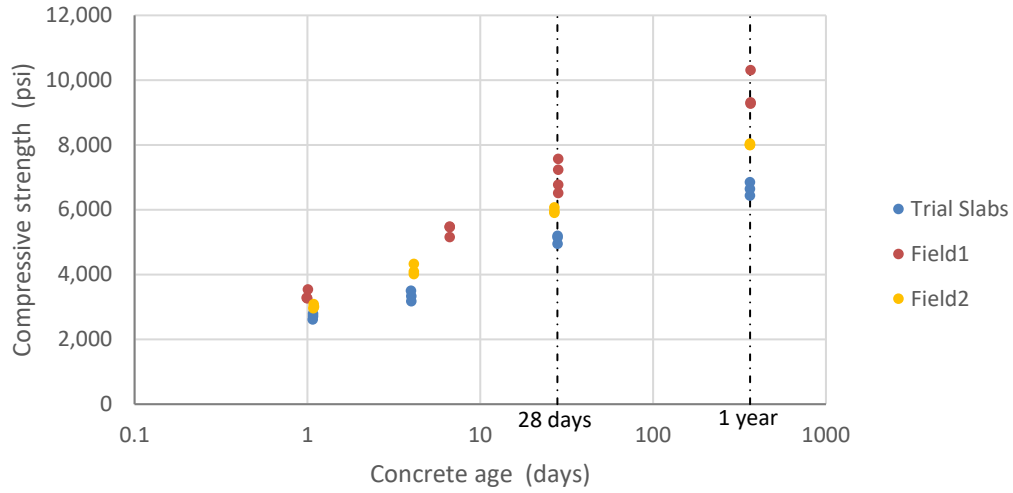


Figure 5.2: Concrete compressive strength.

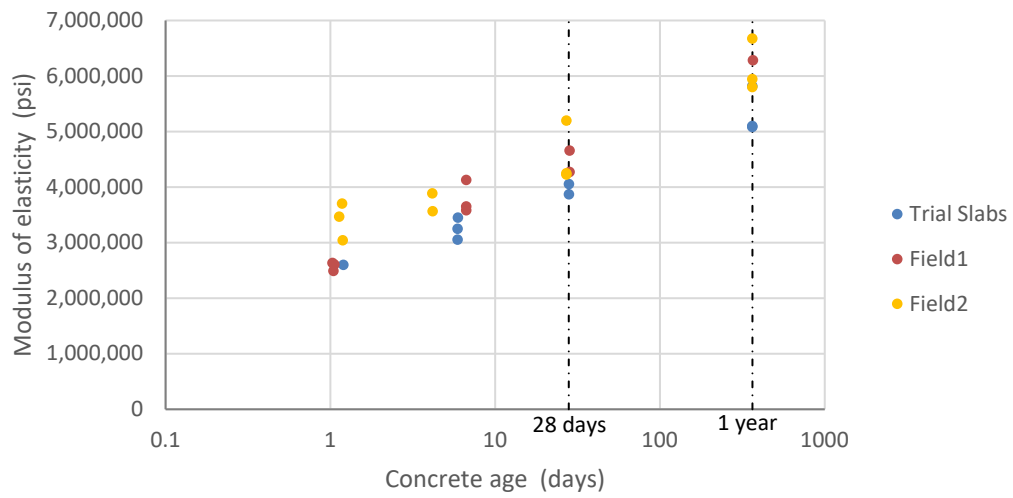


Figure 5.3: Concrete modulus of elasticity.



Figure 5.4: Concrete CTE (at age 42 days).

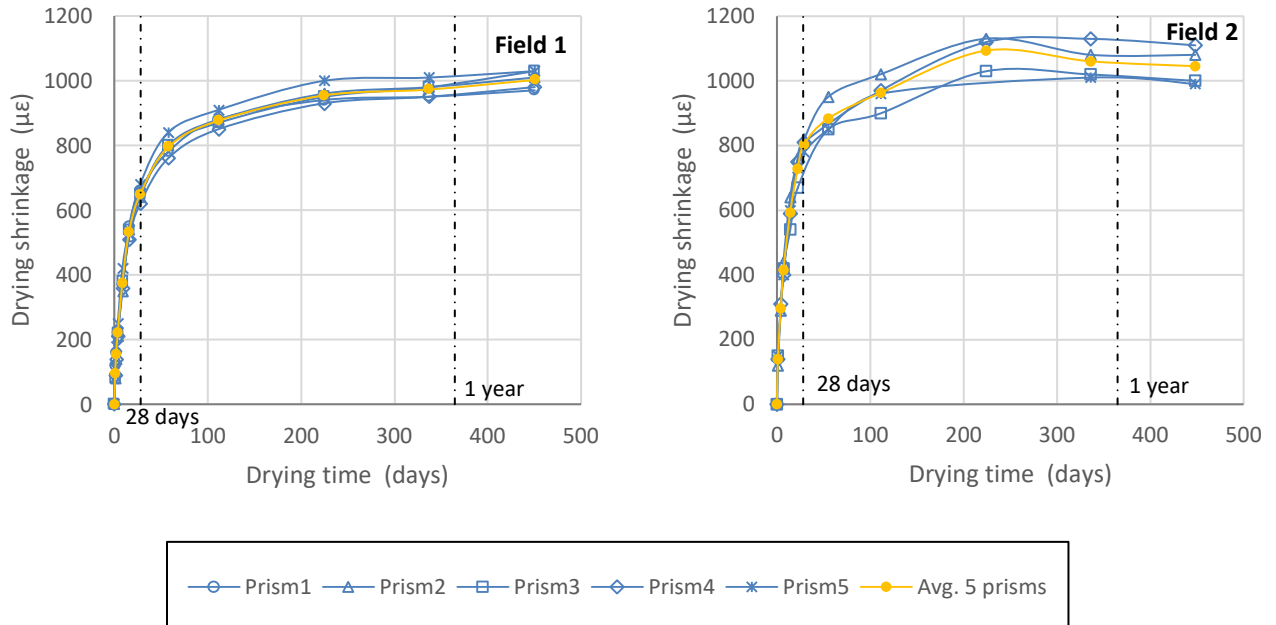


Figure 5.5: Concrete drying shrinkage.

6 SUMMARY, CONCLUSIONS, AND RECOMMENDATIONS

6.1 Summary

This report documents the design and construction of a COA pavement pilot project on State Route (SR) 113 in Woodland, California, one of the first projects where this rehabilitation technique has been used on the Caltrans road network. The project extended over roughly four miles of a two-lane road. The project's northern part, referred to as Segment B (PM 14.760 to PM 17.580), was built in October and November 2018, while its southern part, referred to as Segment A (PM 11.860 to PM 12.890), was built in April and May 2019. A number of the quality control/quality assurance (QC/QA) tests and evaluations summarized in this report were conducted before, during, and after the construction of the concrete overlay.

6.2 Conclusions

The main conclusions from the construction QC/QA tests and evaluations are as follows:

- The asphalt base condition was very poor, particularly in Segment B.
 - After the milling operation, cracking and areas of delamination were present all over the project.
 - At many locations, the milling operation either left an insufficient amount of the original asphalt base or removed it entirely at the shoulder edge of the roadway.
 - It was estimated that the remaining asphalt thickness between the left and right wheelpaths was between 2 and 5 in. in Segment A, and between 1 and 3 in. in Segment B. This remaining asphalt was in poor condition.
- Due to the poor condition of the asphalt base that remained after milling, the Woodland SR 113 overlay is expected to function not as a composite concrete-asphalt structure but as a series of short concrete slabs that rest on the base. None of currently available COA design methods (*Pavement ME*, *BCOA-ME*, etc.) were calibrated for this structural condition.
- The thickness of the newly placed RHMA-G layer varied from 1.2 to 1.8 in., with an average value of 1.5 in. The layer's air void contents varied from 4% to 10%, a range like that observed for the same asphalt mix type in overlays with similar thicknesses.
- Overall, air temperatures were low during Segment B paving, due to the time of the year (October to November) and the nighttime paving operation. During some paving shifts, air temperatures dropped to the freezing point.
- Despite the low air temperatures during Segment B paving, the concrete temperature remained higher than 40°F during the first 72 hours after paving.
- Windy conditions (over 10 mph) affected some of the concrete placements in Segment B's southbound lane.

- Overall, the asphalt surface was adequately wet conditioned before the concrete placement; the asphalt surface was wet but free of standing water.
- Overall, the asphalt surface was not as clean as is desirable for COA construction, and this may have had a negative impact on the concrete-asphalt bonding.
- The asphalt surface temperature varied from the low 30s to the low 70s Fahrenheit during concrete paving.
- Before the concrete was placed, its temperature exceeded 50°F at all times but never exceeded 90°F.
- The tie bars of the longitudinal joints between lanes were inserted manually into the plastic concrete, which resulted in there being little control of the tie bar position and the development of air pockets in the concrete around the manually inserted tie bar.
- The concrete overlay on Segment B was 1 to 3 in. thicker than the 6 in. target.
- Approximately 60% of the transverse joints deployed in two weeks.
- The flexural strength of the concrete mixture after 28 days exceeded the 570 psi requirement considerably.
- The concrete overlay was opened to traffic at least three days after the overlay construction.
- No early-age cracking was observed.
- All the sensors survived the construction of the RHMA-G and the concrete overlay except for one vibrating wire strain gauge and two resistive strain gauges.
- Initial MRI measurements varied from 70 to 175 in./mi. (calculated on 0.1 mi. segments). The information collected for the overlay construction evaluation was insufficient to establish a sure explanation for the high postconstruction MRI.
- Based on slab curvature measurements taken with vibrating wire strain gauges and calculations with *ProVAL*, it is estimated that between 20 and 25 in./mi. of the initial MRI were caused by slab curvature due to drying shrinkage and by temperature gradients.
- The complete concrete surface required grinding due to the poor longitudinal smoothness. Overall, the grinding resulted in a 40% improvement in MRI, though the improvement for individual 0.1 mi. segments varied from 19% to 53%. Post-grinding MRI varied from 50 to 105 in./mi.

6.3 Recommendations

The main recommendations from the construction QC/QA tests and evaluations are the following:

- Before a decision is made about whether to use the COA rehabilitation technique and to proceed with developing a design, it is recommended that a detailed field investigation of the existing pavement that includes a comprehensive coring plan be conducted. The field investigation should focus on both the pavement's lanes and its shoulders, particularly if the use of widened slabs is going to be considered in the design.

- Milling off asphalt that is still in good condition reduces the structural capacity needed to reduce the overlay thickness. The COA technique is more efficient when sound asphalt remains in place, which usually requires no restriction against elevation of the road surface.
- It is recommended that future COA projects specifically address the necessary repairs to the asphalt base after the milling operation.
- It is recommended that future COA projects continue the practice of cleaning the asphalt surface thoroughly before the concrete overlay is placed, as indicated in the Woodland SR 113 rehabilitation special provisions. Additional measures should be implemented to ensure that the contractor fulfills this requirement.
- It is recommended that the special provisions of COA on asphalt projects specifically prohibit the manual insertion of tie bars.
- It is recommended that future COA projects specifically address the need to install dowels in the construction transverse joints.
- The large postconstruction MRI values measured in this project emphasize the need to explore modern techniques like stringless (3D) paving and real-time smoothness evaluation, which may help to achieve smoother concrete surfaces. It is recommended that these techniques be combined with vibrating wire strain gauge measurements to estimate the hygrothermal component of MRI.
- For circumstances where the structural contribution of the asphalt base is expected to be minimal (as was the case with the Woodland SR 113 overlay), it is recommended that consideration be given to expanding the current range of concrete pavement design procedures.

REFERENCES

1. Mateos, A., Harvey, T.J., Paniagua, F., Paniagua, J., and Wu, R. 2019. *Development of Improved Guidelines and Designs for Thin Whitetopping: Summary, Conclusions, and Recommendations* (Summary Report: UCPRC-SR-2018-01). Davis and Berkeley, CA: University of California Pavement Research Center. <https://escholarship.org/uc/item/14t4f662>.
2. Mateos, A., Harvey, T.J., Paniagua, F., Paniagua, J., and Wu, R. 2019. “Accelerated Testing of Full-Scale Thin Bonded Concrete Overlay of Asphalt.” *Transportation Research Record* 2673, no. 2: 404–414. <https://doi.org/10.1177/0361198119825645>.
3. California Department of Transportation. 2005. *Caltrans Pavement Climate Regions*. <https://dot.ca.gov/-/media/dot-media/programs/maintenance/documents/office-of-concrete-pavement/climate/pavement-climateregions-100505-a11y.pdf>.
4. Kim, C., Lea, J., Kannekanti, V., and Harvey, T.J. Forthcoming. *Updating Weigh-in-Motion (WIM) Spectra in PaveM* (Technical Memorandum: UCPRC-TM-2018-01). Davis and Berkeley, CA: University of California Pavement Research Center.
5. Li, Z., Dufalla, N., Mu, F., and Vandenbossche, J.M. 2013. *Bonded Concrete Overlay of Asphalt Pavements Mechanistic-Empirical Design Guide (BCOA-ME): Theory Manual* (FHWA Pooled Fund Project: TPF-5-165). Pittsburgh, PA: University of Pittsburgh. https://www.engineeringx.pitt.edu/uploadedFiles/_Content/Sub_Sites/Faculty_Subsites/Vandenbossche/Documents/BCOA%20ME%20Theory%20Manual.pdf.
6. Mateos, A., Harvey, J., Paniagua, F., Paniagua, J., and Wu, R. 2018. *Development of Improved Guidelines and Designs for Thin Whitetopping: Construction and Initial Environmental Response of Full-Scale BCOA Sections* (Research Report: UCPRC-RR-2017-02). Davis and Berkeley, CA: University of California Pavement Research Center. <https://escholarship.org/uc/item/14t4f662>.
7. Fick, G., Merritt, D., and Taylor, P. 2019. *Implementation of Best Practices for Concrete Pavements: Guidelines for Specifying and Achieving Smooth Concrete Pavements*. Ames, IA: National Concrete Pavement Technology Center. https://intrans.iastate.edu/app/uploads/2019/12/smooth_concrete_pvmt_guidelines_w_cvr.pdf.
8. Voight, G.F. 2002. “Early Cracking of Concrete Pavement—Causes and Repairs.” Paper presented at Federal Aviation Administration Airport Technology Transfer Conference. <http://citeseerx.ist.psu.edu/viewdoc/citations?doi=10.1.1.587.1150>.
9. Mateos, A., Harvey, J.T., Wu, R., Paniagua, F., and Paniagua, J. 2018. *Development of Improved Guidelines and Designs for Thin Whitetopping: Environmental Response of Full-Scale BCOA Sections* (Research Report: UCPRC-RR-2017-03). Davis and Berkeley, CA: University of California Pavement Research Center. <https://escholarship.org/uc/item/14t4f662>.